PROVIDING CONTACT SENSORY FEEDBACK FOR UPPER LIMB ROBOTIC PROSTHESIS

by

Mohammad Aziziaghdam

B.S., Mechanical Engineering, University of Tabriz , 2011

Submitted to the Institute for Graduate Studies in
Science and Engineering in partial fulfillment of
the requirements for the degree of
Master of Science

Graduate Program in Mechanical Engineering

Boğaziçi University

2014

PROVIDING CONTACT SENSORY FEEDBACK FOR UPPER LIMB ROBOTIC PROSTHESIS

APPROVED BY:

Assist. Prof. Evren Samur .....
(Thesis Supervisor)

Assoc. Prof. Burak Güçlü .....

Assoc. Prof. Çetin Yılmaz .....

DATE OF APPROVAL: 07.08.2014

ACKNOWLEDGEMENTS

It would not be possible to finish the thesis without consistent help my advisor, Professor Samur. I sincerely thank him for his guidance which encouraged me to go from vague idea of the thesis to detailed properties of the final tests.

I would also like to thank Prof. Yilmaz and Prof. Guclu for accepting to be member of jury committee despite their overwhelming busy schedule.

I would also thanks our lab members at Haptics & Robotics Laboratory of Bogazici University for encouraging me in the lab.

Finally I would like to thanks my mom for literally everything in my life

ABSTRACT

PROVIDING CONTACT SENSORY FEEDBACK FOR UPPER LIMB ROBOTIC PROSTHESIS

Lack of the sense of touch is the fundamental problem of today's robotic prostheses. Considering the fact that touch feedback plays a significant role in identifying contacted objects, our aim in this study is to use acceleration signals, occurring due to physical contact of a prosthetic hand with objects, as sensory feedback. We apply these signals on the clavicle bone using a tactor as a haptic interface. First, a library of the acceleration signals occurring as a result of tapping on different materials is collected. Effect of the impact velocity is studied and used as a scalar for real-time applications. In order to model the contact accelerations, a stochastic signal model is developed. Due to the distinct waveform characteristics of different materials, the rate of the change of acceleration (Jerk) response signals are used to identify the hardness of the objects. In a human subject study, the whole procedure of recording, identifying and replaying the signals by the tactor is studied. Results of the human subject study showed the ability of the designed tactor to provide distinguishable hardness sensations of different materials in real time.

ÖZET

ÜST EKSTREMITE ROBOTIK PROTEZLERI IÇIN TEMAS HISSI GERIBILDIRIMI SAĞLANMASİ

Günümüzdeki robotik protezlerinin temel sorunu dokunma hissinden yoksun olmalırıdır. Dokunsal geribildirimin temas edilen nesneleri tanımlamada çok önemli bir rol oynadığı bilindiğinden, bu çalışmadaki amaç; protez elin nesnelerle olan temasından ortaya çıkan ivme sinyallerini, duyusal geri besleme olarak kullanmaktır. Bu sinyaller, haptik arayüz olarak kullanılan bir dokunucu sistem ile köprücük kemiğine uygulanmaktadır. Bu tez çalışmasında öncelikle, farklı maddelere vurularak elde edilen ivme sinyallerinden bir kütüphane oluşturuldu. Vurma hızının etkileri araştırıldı ve gerçek zamanlı uygulamalar için bir ölçekleyici olarak kullanıldı. Temas ivmelerini modelleyebilmek için bir stokastik sinyal modeli geliştirildi. Her maddeden elde edilen sinyallerin birbirinden farklı dalgabiçimi olduğu göz önünde bulundurularak; ivme sinyallerindeki değişim hızı, nesnelerin sertliklerini tanımlayabilmek içinkullanıldı. Temas sinyallerinin gerçek zamanlı kayıt, tanımlama ve tekrar oynatılma aşamaları bir insan araştırmasıyla test edildi. Psikofiziksel araştırmanın sonuçları, tasarlanan haptik sisteminin, ayırt edilebilir sertlik hislerini gerçek zamanlı olarak verebildiğini göstermektedir.

TABLE OF CONTENTS

LIST OF FIGURES

LIST OF TABLES

LIST OF ACRONYMS/ABBREVIATIONS

$A(v)$	Function of attack Velocity
B	Magnetic field
B_gL	Force constant of linear motor
d	Diameter of the coil
F	Force produced in voice coil
I	Current
k	Constant of spring
L	Inductance
m	Mass of the moving part of the voice coil motor
n	Number of the wire coils
$Q(t)$	Vibration produced by the contact
R	Electrical resistance
X	Position of the moving part of the voice coil motor
θ_d	Angle between the direction of the current and the magnetic flux
ω	Frequency of the attack portion of the waveform

1. INTRODUCTION

1.1. Motivation

Human body interacts with the external world with the five senses. Sight (ophthalmoception), hearing (audioception), smelling(olfacoception), taste(gustaoception) and touch((tactioception) are sensory modalities that play a dominating role in perception of surrounding enviroment. Sense of touch is based on the somatosensory system in our body, which works when an activity in a sensory neuron is triggered by an external stimulus such as vibration on the skin [1]. According to Juhani Pallasmaa "touch is the most primary experience in architecture because the senses of the skin are the mediator between the skin and the world" [2]. Touch as natural sensory feedback mechanism plays a great role in understanding physical properties of objects in contact and also let us to accurately manipulate them. In addition, calibration of grasping and pinching force, recognition of the shape of an object and knowledge of the position of the hand in space contribute largely to such dexterity that we take for granted [3].

Loss of touch sense could be because of losing a limb like hand. In this case. usually a prosthetic device is used to make the person with limb loss to do some tasks easier. The number of tasks as well as their convenience is related to the type of the prosthetic device that is used. A prosthetic device could be a simple one with no movements in parts, or a robotic prosthetic device which could imitate movements of a natural limb. Recently many studies have been done on designing robotic prosthetic devices which could imitate a real hand's movements [4]. Controlling such devices basically done by translating some unrelated movements into intended movements in arm or fingers (for example moving shoulder to open or close the artificial fist) [5]. However, even for an accurate robotic prosthetic device which provides fine movements, lack of sensory feedback could make difficulties in controlling the device. Although new methods, like electromyography (EMG) [6], has been used for controlling prosthetic devices

recently, lack of sensory feedback for such devices still is a problem which sometimes yields to rejecting those modern prostheses by users [7]. Furthermore, another problem that users of such devices face with is the lack of awareness about the existence of their prosthetic device [4]. A proper way to solve these issues in using robotic prosthetic devices is to maintain sensory feedback for theses devices which makes the users to have a tactile feedback through their prosthesis. Using a sensory feedback mechanism in prosthetic devices not only helps user to accept a robotic device as a part of his/her body but also enhances its controlling and reduces the time that user needs to make a vision contact with his/her prosthetic device while using it [8].

Advancement in both hardware and software technologies in recent years made steep rise in interest for creating new types of prosthetic limbs. In the last fifteen years different robotic prosthetic limbs has been produced which are compatible with human anatomy and able to resemble the natural hand movements [9–16].Despite major technological progress in producing such devices, prosthetic devices are still far more limited than human hand in terms of control, amount of sensory feedback provided and methods of classifying different grip patterns and motions [17].

Introduction of control using Electroneurography [1] (ENG) and Electromiography [2] (EMG) created a great opportunity for development of more advanced robotic prosthesis . The first motoriezed prosthesis which used myoelectric signals as control element has been developed by Battye *et al.* in 1955 [19]. It has been reported that the primary disadvantage of prosthesis controlled by myoelectric signals is the lack of sensory feedback [20]. In order to solve this problem a supplemental sensory feedback is used to restore the lost sensation. Supplemental sensory feedback refers to information which is conveyed to the person with limb loss, about the state of the prosthesis [21].

[1] A prosthetic hand controlled by ENG is operated by electrodes interfaced directly with the peripheral nervous system or the central nervous system. Interfaces with the PNS have been used for two major applications: functional electrical stimulation (FES) and the creation and control of artificial limbs [18]

[2] A myoelectric prosthesis uses electromyography signals or potentials from voluntarily contracted muscles within a person's residual limb on the surface of the skin to control the movements of the prosthesis [18]

1.2. Background of Sensory Feedback for Prosthesis

A prosthesis using sensory feedback could be thought as a system with close-loop control [22]. Function of a prosthesis would be better with a close-loop control, if they use both exteroceptive as well as proprioceptive information [23]. There are two potential ways to elicit sensory feedback after losing the receptors of skin due to limb loss, invasive and noninvasive. In case of invasive method the sensory cues captured in prosthesis sent directly to physiologically relevant neural structures in the peripheral; neural system or the Central Nervous System (CNS). On the other hand in noninvasive method the sensory feedback is provided on an intact sensory system(e.g., tactile stimulation on residual limb) [24].

Two common methods of noninvasive sensory feedback are electro-tactile and vibro-tactile stimulations [25, 26]. Electro-tactile stimulation or electrical surface stimulation is a method where muscles nerves are stimulated by an electrical pulse in order to convey feedback of sensed action. Electrical stimulus can be delivered directly to the neural tissue to generate the desired response of the nerve [23]. Electro-tactile devices consume less power and respond faster than vibro-tactile devices because there are no moving mechanical parts. Another advantage of electro-tactile stimulation is that it allows 59 different sensations [27]. Shannon has used strain gauges to provoke an electrical stimulation as sensory feedback [28]; in this a series of pulses had been used and pulse repetition rates were modulated with pinch force sensed by prosthesis. Even though this method increases the functionality of the robotic prosthetic devices; it also faces with critical issues. One of the limitations of electro-tactile stimulation is the physical incapacity of this method to selectively stimulate the Pacinian corpuscles in the deeper tissue without the activation of the shallower receptors [29]; the main drawback of this sort of stimulation is interference with myoelectric control when stimulations area is close to EMG electrodes [30, 31]. In a study done by Paciga *et al.* [32] it has been reported that interference of EMG and Electro-tactile stimulation signals could occur inevitably; however, this method is still an option if the feedback system

is placed at least 60 mm away from the pick-electrods of EMG.

Vibro-tactile stimulation is a method which uses a mechanical device to stimulate Cutaneous Mechanoreceptors [3] [33]. Vibro-tactile feedback in prosthetic devices was firstly introduced by Conzelman *et al.* in 1953 [34]. This method's compatibility with EMG control and higher acceptability compared with electro tactile stimulation are the reasons which made vibro-tactile stimulations to be explored more than other methods [25, 27]. In a concept proposed by Bach-Y-Rita and Collins arrays of vibro-tactile stimulators convey proprioceptive information on the back or on the residual limb of the person with limb loss [35]. In another concept for kinesthetic data of the prosthesis introduced a system where the elbow angle of Boston Arm was feedback using vibro-tactile stimulators [36]. Vibro-tactile method generally improves the performance of the prosthetic devices through better control of grip and by lowering the number of the errors in task executation [37]; however, there are some flaws in this method such as capability of providing lower sensations and being bulkier than electro-tactile feedback devices [33].

1.3. Contribution of The Thesis

The purpose of this study is to find an efficient sensory feedback method which would convey contact feeling to a user of robotic prosthesis. In order to achieve this goal a tactor has been designed to be attached on an intact part of the body.

It has been shown that high frequency acceleration response signals due to tapping on different materials contains important cues which helps human to detect the hardness or softness of the contacted materials [38]. By playing spectrum of these signals we aim to provide various hardness sensations on clavicle bone Figure 1.2. The designed tactor will play set of acceleration signals which have been collected by tapping on different materials with a mechanism that we have designed. Although using

[3] Cutaneous Mechanoreceptors are free nerve endings, sensing touch, pressure, and stretch. They are classified into four main types in the human skin shown in Figure1.1 [33]

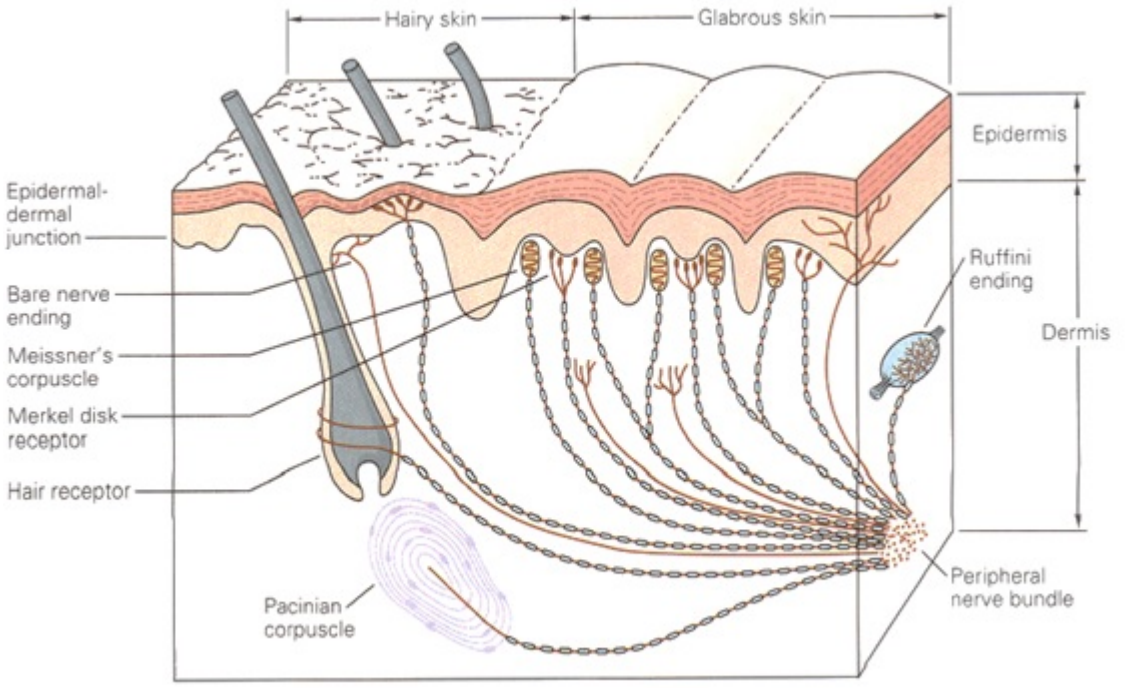

Figure 1.1. The morphology of mechanoreceptors in hairy and hairless (glabrous) skin of human [10].

a tactor as a haptic interface has been proposed before [29], we believe that adding high frequency acceleration signals could improve the contact realism and therefore the control of prosthesis. To the best of our knowledge, sensory feedback through high frequency accelerations has never been applied to prosthesis before. In order to fulfil the described requirements, the below aims have been followed:

Aim 1: To gather the acceleration signal generated in physical interactions of a prosthetic device with different materials. This has been done by designing a stylus and recording accelerations applied on stylus while tapping it on different objects.

Aim 2: To design a haptic device for transmitting acceleration signals to prosthesis users. The acceleration signals was based on the contact data obtained in aim 1 and mapped to the haptic device, so that meaningful information will be given to the users. A mechanism has been designed in a way which we could impart the signals on

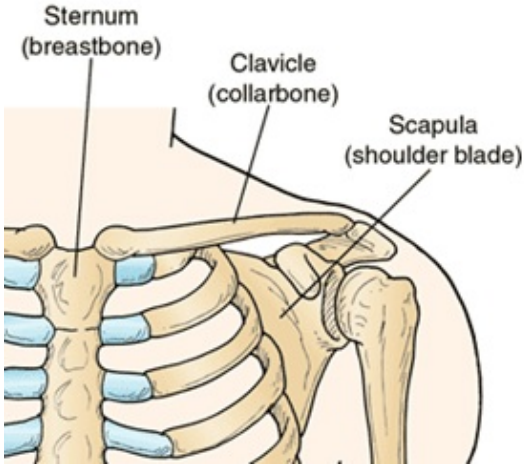

Figure 1.2. Clavicle bone [10].

clavicle bone in the shoulder.

Aim 3: To investigate whether rich tactile information such as feeling of texture, shape of the touched object and slippage detection while holding an object, could be conveyed by the designed haptic device.

2. LITERATURE REVIEW

In order to cover the aims noted in Section 1.3, related studies has been reviewed. This chapter contains abstract of important related studies which help us in different steps of the research.

2.1. Vibro-tactile Feedback

Vibro-tactile haptic feedback had been used in different areas and systems, such as gaming, virtual-reality, tele-robotics, Human-Machine Interface (HMI) and prosthetic devices. This method has been used to fedback variety of modalities.

In case of virtual reality different studies have been conducted to make the haptic feedback more realistic and acceptable. For instance, a study has been conducted by Okamura *et al.* [39] in which by using a stylus (joystick) realistic vibro-tactile feedback of different materials had been generated. In this research force, velocity and vibration of a stylus had been gathered while tapping on materials, stroking textures, and puncturing membranes. In this study the contact signals had been modeled as a decaying sinusoidal signals. It has been shown that adding vibration to different sensation feedbacks could increase the perception of the task done in virtual environment. In a similar study using SensAble's Phantom [40] vibration feedback used in virtual environments with reality-based models [41]. In this study a modified reality-based vibration parameters had been proposed through a series of perceptual experiments with a haptic display. By recording the acceleration due to tapping on different materials, a decaying sinusoidal model of the signals had been developed and used as vibrational feedback in virtual environment. Contact acceleration data had been used in order to create realistic virtual texture in a study by Romano *et al.* [42]. In this study a handheld tool had been used to capture the acceleration, position and force of the tool while interacting with different textures; in order to render the textures on

a Wacom tablet an stylus augmented with small voice coil actuators had been used. Also other studies have been done to produce different models and environments using vibro-tactile method [43, 44].

In the area of the tele-operation vibro-tactile feedback has been used to maintain a tactile feeling of a remote robot. In a study done by Massimino *et al.* [7] vibro-tactile feedback used to transmit the force information applied on a remote manipulator. Vibration display had also been used to convey specific data such as detection of looseness in an assembly of parts or damage to a ball bearing [45]. In this study in order to provide high frequency vibration display, a voice coil with range motion of 3mm was used which had the ability to produce 0.25 N at 250 Hz. In case of robotic surgery an study has been done by McMahan *et al.* [46] where a sensing and actuating device that can be added to Intuitive Surgical's existing da Vinci S Surgical System to provide auditory and vibro-tactile feedback of tool contact accelerations. With this method surgeon could both hear and feel the acceleration signals produced due to contact with rough textures and also contract with objects and other tools. In order to recreate haptic feedback of surgical robot's tool acceleration, voice coil motors (Figure 2.1)were assembled on the da Vinci S Surgical System. It has been show that even though high frequency acceleration feedback can not directly provide force information, it could convey the contact and roughness data of objects which surgical tool is interacting with. Considering surgery Yao *et al.* [47]a surgery robot had been enhanced to provide haptic feedback of tissue anomalies while doing minimally invasive anthropoid. An accelerometer and actuator was attached to a probe. The function of the designed system was to magnify the accelerometer values recorded while doing the surgery and play them by using actuators. Other studies [48, 49] also show the effectiveness of using vibro-tactile feedback in both perceiving the sensation and controlling the remote robot.

Since robotics prosthetic devices had been in it's first steps of development, lack of the sensory feedback in these devices was a big issue which was making of these devices

Figure 2.1. Voice coil motors used for surgical robot in [46].

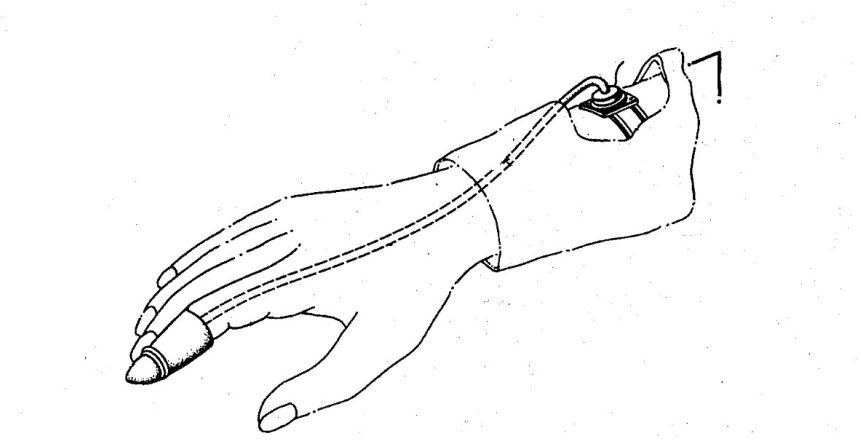

Figure 2.2. First sensory feedback system for prosthetic arms [34].

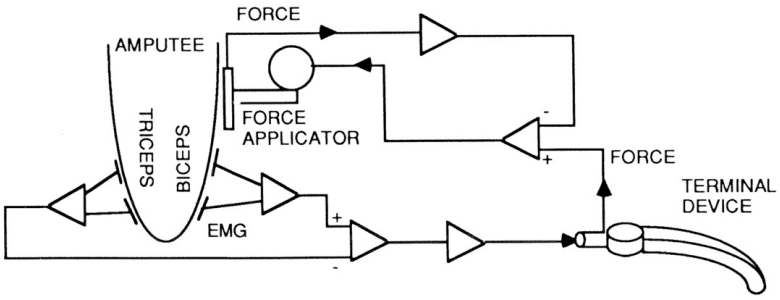

Figure 2.3. Sensory feedback system developed by Meek *et al.* [51].

to face with problem of control and manipulation [50]. The idea of using a sensory feedback on prosthetic devices has been first announced as a patent by Conzelman *et al.* [34]. In this study they had used a hydraulic system where the pressure on the tip of the finger s where transmitted to another area of the body using veins (Figure2.2). Later in research done by Meek *et al.* [51] the force applied by the prosthesis's fingers in a grasping procedure was reproduced on the residual limb using a mechanism driven by a rotary motor. In this study the designed EPT (Extended Physiologic Taction) system could apply the force on the skin of the operator proportional to the grip force of the prosthesis. Similarly it could also transmit to the user, vibrations which occurred while interacting with different objects with the prosthesis. As shown in the Figure 2.3 the system consists of a motor and a force applicator which applies force and vibration on the residual limb of amputee. The results of this study show the ability of this system to improve the grasping control in prosthetic devices. It also shows the sufficient matching of vibro-tactile feedback with EMG controlled prosthesis.

Pylatiuk *et al.* [52] showed that using a simple eccentric vibration motor could increase the control of the prosthetic devices and also lower the force needed in comparison with other methods used as vibro-tactile devices. In this study a simple force sensor, FSR (Force-Sensing Resistor), is used to measure the force on the tip of the fingers of the prosthetic device. The sensed force signals then used as a actuation signal for the vibrational motor; as the force increases the motor vibrates faster (or with higher frequencies) proportional (Figure 2.4). They demonstrated that using this device and transmit the vibrations directly to the skin could decrease the force needed

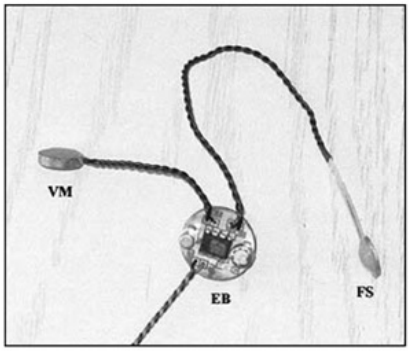

Figure 2.4. Simple vibro tactile feedback using FSR and vibrational motor [52].

to grasp object by the rate of 57% .

Chatterjee *et al.* [53] argued that using vibro-tactile feedback could only have a significant effect for people who have experience in using EMG control prosthesis. In their feedback system they have used a C2 tactor of Engineering Acoustic Inc, which was mounted to the upper arm of the user with an elastic band. They have used square wave signals as stimulation. The signals were modulated with both an envelope and a carrier frequency as shown in Figure 2.5. Using train of discrete vibratory square waves, the grip forced is conveyed; slower pulses represented as weaker grip force and rapid pulses were represented as stronger. Strain gauges were used to measure the force and these force information were then fed to the tactor proportionally, in which higher envelop frequency correlated with higher grasping force. The carrier frequency changes between 100 Hz to 230 Hz relevant to the position of the hand; using this method some proprioceptive information is conveyed to the user of the device which could be helpful in adjusting the position of hand and fingers without need of vision. Even though using this system helped the users, it was shown that improvement in control of such devices was significant for users with experience in using EMG controlled prosthesis.

One of the most comprehensive designs of vibro-tactile devices done by Kim *et al.* [29] in which they have included multiple modality feedback in their design. Their design which was especially for people who have undergone targeted nerve reinnervation

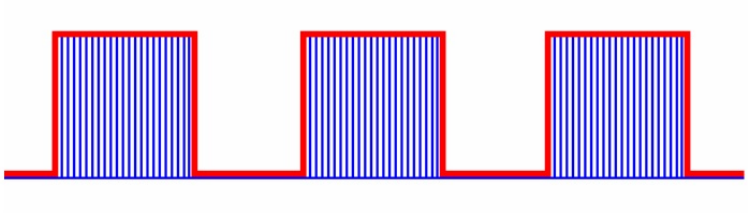

Figure 1: Sample vibratory stimulation waveform: envelope frequency shown in red, carrier frequency in blue.

Figure 2.5. Wave form used for stimulation [53].

surgery [4] is able to display contact, pressure, vibration and shear force. In this study two different mechanisms (five bar and six bar mechanisms)were chosen to design the tactor (vibro-tactile device). Five bar mechanism has been chosen for its simplicity; however, due to its limitation in picking link lengths which could provide sufficient workspace it has been eliminated. Therefore they have designed two different types of six bar mechanisms; a gear constrained mechanism which was similar to a five bar mechanism (Figure 2.6a) and its tactor head is always parallel to the skin. A negative point for this kind of mechanism is undesirable friction between the gears. The second type is a six bar skewed parallelogram mechanism (Figure 2.6(b)) which even though it doesn't face with the problem of friction in geared mechanism, the complex design of this type of tactor makes other problems such as link collusions, backlash and over constraints. In order to drive the mechanism three different kinds of Maxon Motors have been used. Moreover, to make a close loop control of pressure, vibration and shear force custom made strain gauge sensors were developed. The psychophysical test that they have done with two TR patients showed the capability of their tactor in discriminating between three different textures. Patients were 91% and 96% correct in discriminating between sandpaper, Teflon and Ribbon. Even though this system is working well, it seems to be a little big considering importance of the sensations. In other words, since their patients prioritized the feeling from most to least important

[4]Targetted reinnervation surgery is a method in which nerves of spare muscle of an amputated patient is cutted and/or deactivated and reinnervation with the residual limd of the patient. With this method the EMG signals of the targeted muscles will now be present in the muscles which nerves had been innervated to; therefore the new reinnervation limbs could be used both for control and receive the feedback of the robotic prosthetic devices [54].

as : contact, pressure, temperature, vibration and shear and considering the fact that touch and pressure are the most important sensations, such big device does not seem to be efficient. As they have reported in their study they will try to make it smaller to make it more reasonable to use as sensory feedback device. From another point of view considering every amputated patient to undergo the TR surgery to be able to use this type of device dosen't look like a feasible approach.The six bar gear constrained mechanism shown in Figure 2.6(a) also had been used in another study [55] in which a complete psychophysical test had been done to analyze the functionality of this type of sensory feedback device.

Combination of eccentric motors have been used by Ciprianni *et al.* [56] to provide vibrations with different magnitude and frequency as well as beat interference. As shown in Figure 2.7 two different placement of eccentric motors were used to make the system provide vibrations with variety of frequencies and amplitudes. Two different subjective tests were done; first was just to test the amplitude discrimination and second was to test the combination of frequency and amplitude. In the first experiment by using comparison of three different combinations of motors the subjects were just tested to see if they could discriminate the difference in the amplitude. In this part the frequency of the motors were constant in the range of 156 Hz maximum and 122 Hz minimum. In the second part since both frequency and vibration of the motors change with current at the same time, motors were on and off with different orders. Results of this study showed the fact that frequency and amplitude of the vibration has to change coherently in order to reach to maximum discrimination by the users.

In 2012 an study done by Witteveen *et al.* [57] demonstrated the advantage of using vibro-tactile feedback on proprioception. In this study opening and closing position of the the hand was feedback on the forearm. The stimulaters were placed in two different compositions as shown in Figure 2.8, longitudinal orientation and transversal orientation. Eccentric coin motors were used as vibro-tactile feedback. Electro-tactile feedback was provided by small surface electrodes. The distance between the stimu-

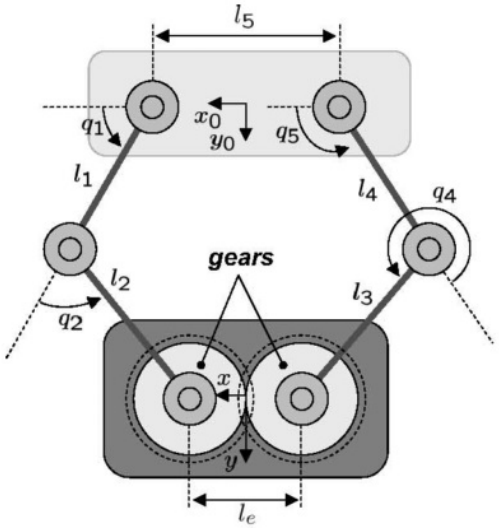

(a) Six bar gear constrained mechanism.

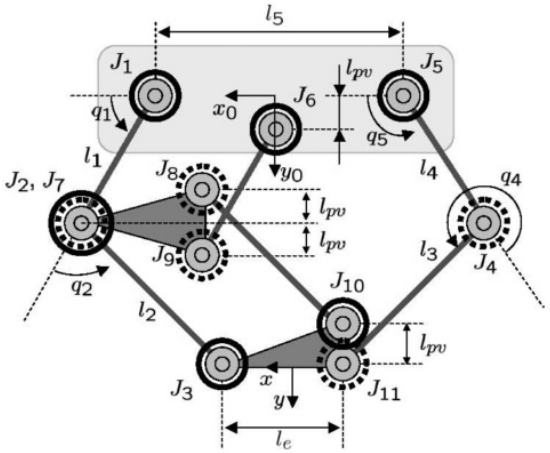

(b) Six bar skewed parallelogram mechanism.

Figure 2.6. Mechanisms designed to provide multimodal sensory feedback for prosthetic devices [29].

laters were 39 mm for longitudinal and 38 mm for the transversal orientation. In their subject test they have given the feedback to the arm. The same arm also was used to do the experiment with. The results showed that there were no significant different between the orientation of the stimulaters. Generally it has been shown that for every different position the vibro-tactile stimulation feedback was significantly better and the grasping function was better using this kind of feedback in comparison with electro-tactile feedback. Also it has been demonstrated that adding more vibro-tactile

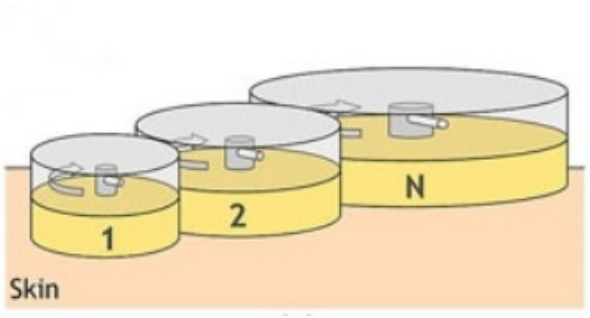

(a) Planner composition of motors.

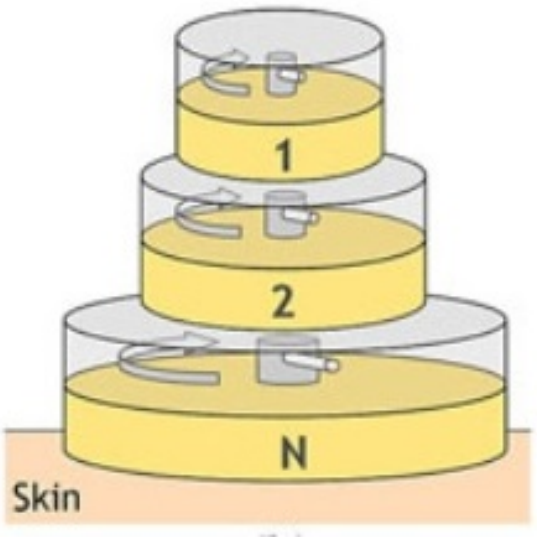

(b) Coaxial composition of motors.

Figure 2.7. Two different composition of eccentric motors used in [56].

stimulaters will to the efficiency of the grasping and proprioception, however, adding more electro-tactile stimulaters had no effect on efficiency of the position feedback and grasping function.

In a study done by Domian *et al.* [58] a single actuator wearable haptic device was used to relay the force and slip speed. As shown in Figure 2.9 the haptic device consist of a normal force transmission belt and also a slip speed transmission belt. This device is able to generate the normal force 1.5 to 5 Hz and slip speeds in the range 50 to 200 mm/s. In order to measure the capability of the device in transmitting the haptic modalities (Force and slip speed) two experiment has been conducted. In the

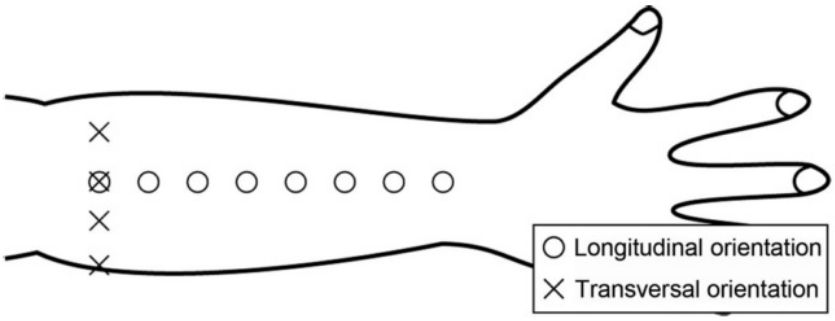

Figure 2.8. Different orientation of stimulaters on the forearm [53].

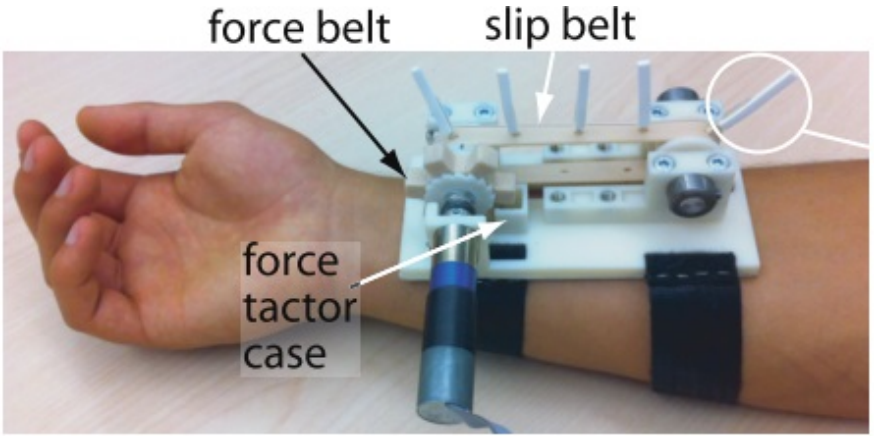

Figure 2.9. Single actuator wearable haptic device [58].

first experiment participants were just given the force feedback after a training phase; in training phase participants were given different levels of force until they became confident about their choice on the stimuli level. The second experiment includes both force and slip speed feedback. It has to be noted that in this device the sensations were fedback one to one; in other words force given by the haptic device was demonstration of the force in grasping and slip speed was demonstration of the slipping speed if the grasped object slips while grasping. The results of the experiments showed that the force was better perceived by the user in comparison with slip speed. The authors also suggested that longer training sessions could improve the perceived sensation; however, long training sessions could be considered as a negative point for a haptic device.

2.2. Signal Modeling

In every different robotic device sensors are used to capture the information about the environment which the robot is interacting with. In the area of the haptics also sensors, whether force or acceleration sensors, are used to record the data of force or acceleration occurred in variety of functions. Collected data from sensors need to modeled. Data modeling is helpful in having a controlled experiment. Further more it will be also helpful in signal identification procedure.

Considering materials as a mass-spring-damper system shown in Figure 2.10, tapping response of materials could be interpreted as impulse response of mass-spring-damper system. Impulse response of single degree of freedom mass-spring-damper system is shown in Equation 2.1

$$x(t) = \frac{F}{m\omega_d} e^{-\xi\omega_n t} sin(\omega_d t) \tag{2.1}$$

where x is the displacement of mass, F is the force, ω_n is the natural frequency, ω_d is the damped frequency and ξ is the damping ratio.

In the area of the haptics different modeling approaches were used to make a mathematical representation of the signals. In an study of Okamura *et al.* [39] exponentially decaying sinusoidal model was used to model the signals that have been recorded by their experimental setup. Using a tapping mechanism they have recorded the acceleration occurred by tapping on different materials. The model that has been used in this study is as below:

$$Q(t) = A(v)e^{(-\beta t)} sin(\omega.t) \tag{2.2}$$

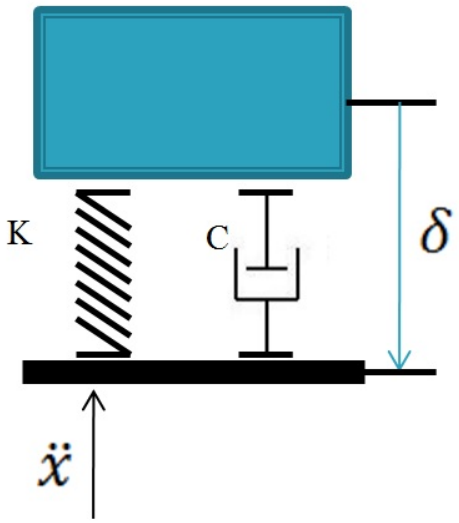

Figure 2.10. Mass-spring-damper system.

where *Q(t)* is the vibration displacment produced by the contact, *A(v)* is a function of attack velocity and β is a constant picked to match the decay envelop of the wave form and ω is the frequency of the attack portion of the waveform. The results of this study showed that the attack amplitude which is the maximum of *Q(t)* during the first cycle, changes linearly with the attack velocity. Another fact which was shown in their results about the characteristics of the signals and their model was that frequency of the signals increases as the stiffness of the tapped materials increase; however, they couldn't find any predictor for their modeling by parametrization of their signals' models. Due to this problem the frequency criteria of the signals were just limited to the signals of the material which they have done the experiment.

In another study at 2001 [41] vibrational parameter models have been explored. In an study which has been conducted through a series of perceptual experiments the effect of these parameters have been explored. The model that has been explored in this study as previous study was the sinosiodal model of the acceleration signals. Frequency, amplitude and decaying rate of the different material's acceleration response, due to tapping, has been collected. As it is shown in the Figure 2.11 the signal preparation in this study contains model of measured signal and a scaled model of the signal based on the bandwidth of the device and the human body sensitivity. As noted the model

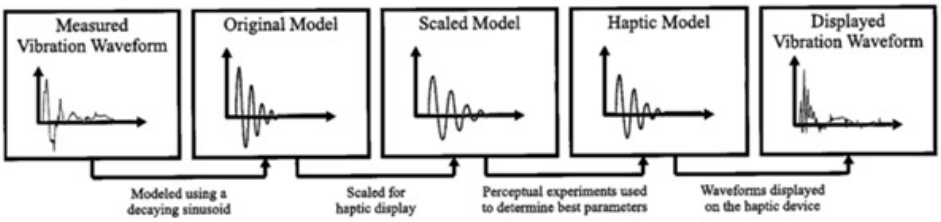

Figure 2.11. Measured and modeled vibrational waveforms [41].

that has been used in this study as similar to the previous one; the first parameter of the formula, A(v), was measured by multiplication of attack velocity and a scalar. The decaying parameter (β) was found by least square method which was fitted to the positive and negative peaks of the waveform. Finally the frequency parameters of the model ω was determined by taking Fast Fourier Transformation (FFT) of the signal. It has been reported in the study that frequency content of the signal does not change until a moderate change in the velocity of the attack.

Kuchenbecker *et al.* argued that adding high frequency transient forces could significantly improve the realism of contact in comparison with traditional force feedback. It has been reported that scaling decaying sinusoidal models by attack velocity could resemble the feeling of real impact. Moreover by doing series of psychophysical tests they have showed that by displaying transient signals the virtual objects feel more like real objects while using traditional force control the virtual materials feels softer than the normal ones.

Further more, in some studies [38,46,59] instead of modeling, filters has been used to make a one to one feeling between actuation signal and sensed signal (captured by the sensor). In such methods by using mathematical formulas or hardware electronic parts, the desired part of the captured signals is trimmed from the rest of the signal and by scaling the magnitude it is fed to the actuators in the haptic devices. This method could have acceptable perceiving rates if the position which the haptic modality is fed has a relation to the position in which the sensation is captured by sensor in remote robot or device.

3. CONTACT ACCELERATION DATA

As noted in literature review in Chapter 2, multiple researches demonstrate the effective manner of the acceleration response signals in providing realistic feeling of contact with objects. Motivated by these studies we aimed to use acceleration response signals in order to provide contact feeling for robotic prosthetic devices.

3.1. Measuring Acceleration Response Signal

In order to understand the characteristics of acceleration response signals which occurs due to contact with different materials, first these signals have to be collected and explored. To capture the acceleration response signals of different materials a mechanism has been designed. The mechanism that we have chosen for this purpose is Hoeken mechanism [60]. We have chosen this mechanism because of two basic reasons. Firstly, we needed a mechanism to provide constant linear velocity in order to explore the effect of the attack velocity in acceleration response signals. Since this mechanism provide a linear constant velocity with rotary actuation, it was a nice fit considering desired design parameters. The second reason that we have chosen this mechanism is the simplicity of designing and producing this mechanism.

First draft of the mechanism was designed using MSC.ADAMS Software. As seen in the figure below the the mechanism has been designed and appropriate lengths of the links and joints were measured (Figure 3.1). Simulation of the mechanism also shows the capability of the designed mechanism to provide constant velocity or zero acceleration. As shown in the figure 3.2 the coupler point of the mechanism goes through a constant velocity. Also the acceleration of the coupler point became almost zero in the same zone (Figure 3.3). In order to measure the attack velocities effect on the acceleration response signals this point was chosen as attack point. In other words the objects were placed in this point and the coupler point of the mechanism

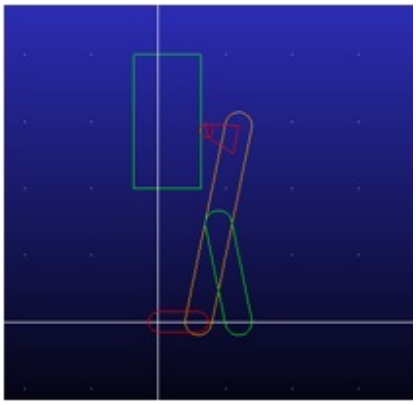

Figure 3.1. Designed mechanism in MSC.ADAMS Software.

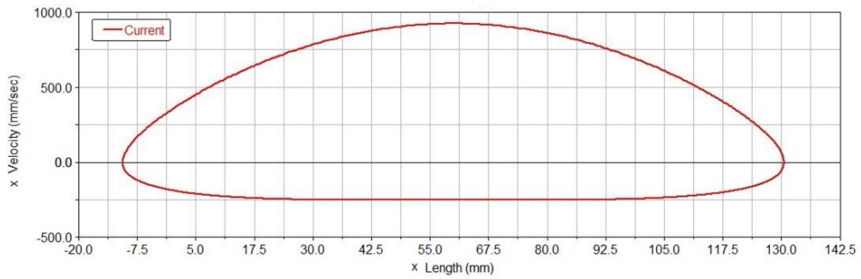

Figure 3.2. Coupler point velocity vs position.

contact with the object in this point. Designing and simulating the mechanism help us to distinguish the mechanism parameters.

As shown in Figure 3.4 mechanism has been designed with details in CATIA. As shown in figure 3.4(a) ball bearing have been used in order to have smooth motions. Drawn cup needle roller bearings with open ends (HK0609) has been used for the joints between the links. The dynamic load rating of this bearing is C_r=2.85 kN and it's static

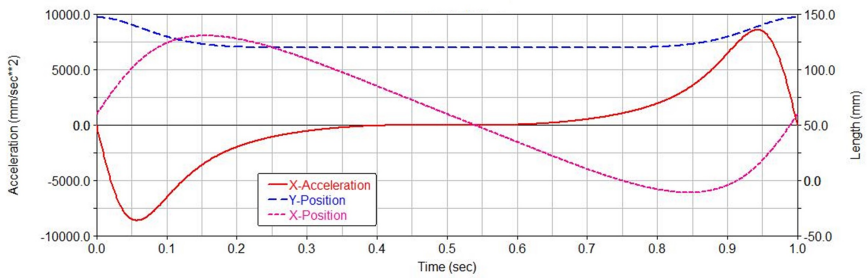

Figure 3.3. Coupler point acceleration and position vs time.

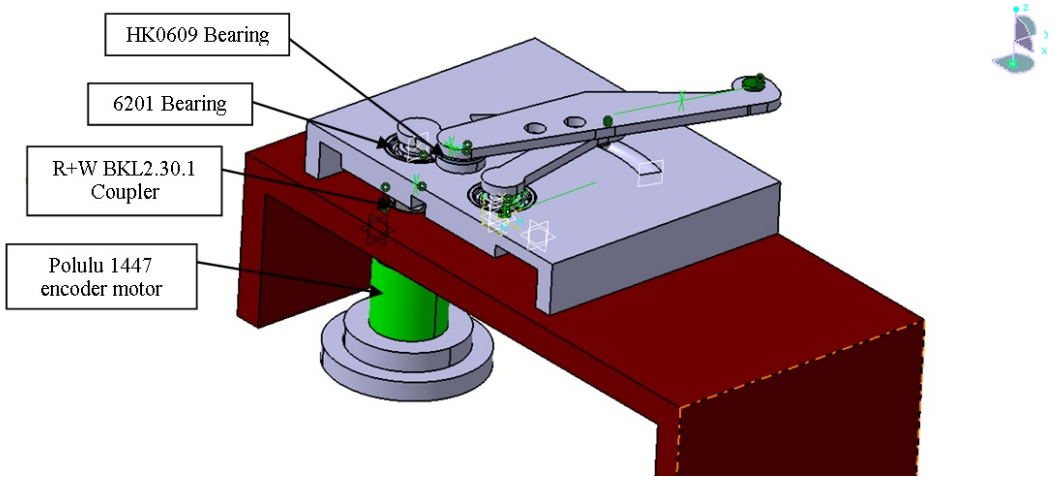

(a) Mechanism parts.

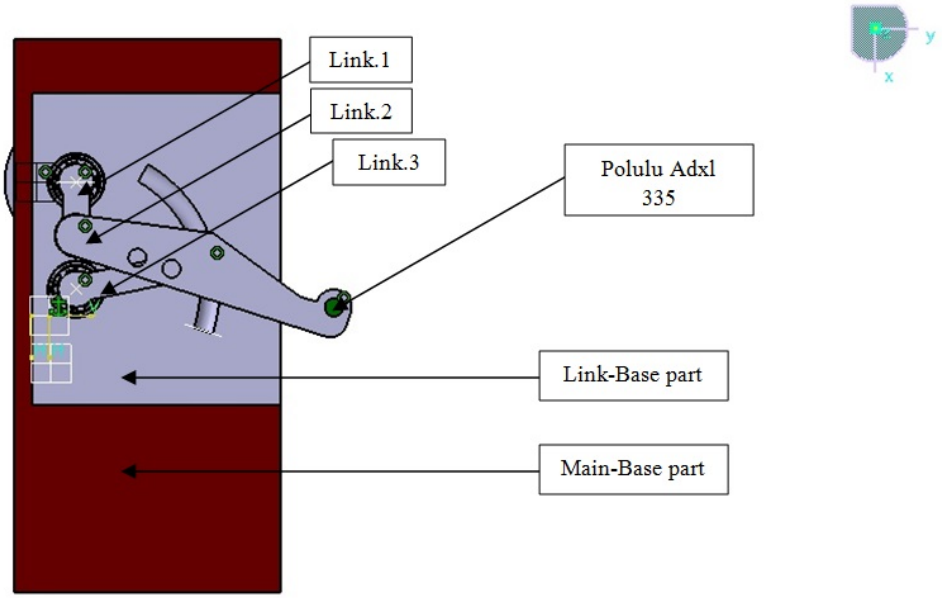

(b) Top view.

Figure 3.4. Data recording setup.

load rating is C_{dr}= 2.6 kN. The outside diameter is 10 mm and the inside diameter is 6 mm (Appendices A). Also in the joints between the link part and and the link base part 3.4 single row deep groove 6201 SKF ball bearing has been used. For this bearing the dynamic load rating is C_r=3.3kN and it's static load rating is C_{dr}= 3.1 kN. The outside diameter is 32 mm and the inside diameter is 10 mm(Appendices A).

In order to couple the shaft of the DC motor (Actuator of the mechanism) and link.1 as driver link of the mechanism (Figure 3.4) R+k BKL 2.30.1 coupler has been used. The feasibility of this coupler compensate the miss alignment which could occur while assembling the parts. Further explanation about the coupler is described in Appendices A.

As noted above polulu 1447 encoder motor was used. This gear-motor is a powerful 12V brushed DC motor with a 131.25:1 metal gearbox and an integrated quadrature encoder that provides a resolution of 64 counts per revolution of the motor shaft, which corresponds to 8400 counts per revolution of the gearbox's output shaft. The stall current of the motor at 12V is 5 A and it's stall torque is 1.76 N.m. Also at 12V the free run speed is 80 rmp. The physical dimensions of the motor is represented in APPENDIX A. The encoder of this motor is a magnetic hall sensor. Hall sensor are solid state devices which are popular due to their non-contact wear free operation, their low maintenance and robust design. As a magnetic field passes over semi-conductor film, a very small magnetic field passes through the semi-conductor making an edge pulse in the device. Using these pulses the position, velocity and direction of the movement of the motor could be measured. In order to control the DC motor first motor model has to be found. First order model of DC motor was chosen as shown in Equation 3.1 [61]

$$G(s) = \frac{b_0}{a_0 + a_1 s} \tag{3.1}$$

where b_0, a_0 and a_1 are model parameters. Using different signals as input, the model parameters were defined by least square model. The model parameters were $b_0 = 61.50$, $a_0 = 1$ and $a_1 = 1.083$. Found model helped us to in designing a PID controller for the DC motor. Using Matlab Control System Design and Analysis toolbox the parameters of PID controller were driven as $K_p = 0.088$, $K_i = 0.16$ and $K_d = 0.0015$. With designed PID controller DC motor's step response information became as *Rise*

Time = 0.343 sec with *Over Shoot* of 6.15%.

Arduino Uno is a microcontroller integrated circuite based on ATmega 328 microcontroller. It has six PWM (Pulse Width Modulation) port and six analog ports with sixteen MHz resonators. It's operating voltage is 5 volts and it's input voltage limits are between 6 to 20 volts. Arduino Uno is able to communicate with computer with TTL (Transistor Transistor Logic) as a serial communication. Benefiting from ATmega16U2 the serial communication could be done through a USB port which appears a s a com port on the computer. It could be both programmed it's own C base interface or useing the pin-wise communication by computer with MATLAB. However, since the USB communication isn't a realtime communication and confronts with delay, Using ATmega 328 microcontroller as programming base device is considered in this study.

In order to amplify the PWM signals which are used to run the motor a dual H-bridge motor driver IC (DRV8833) has been used. Out put voltage of DRV8833 is between 2.6 to 10.7 volts with 0 to 1.2 A continuous current. Communication with this 16-bit IC pins could done by 250 kS/s.

In this study ADXL335 analog accelerometer was used. The measurement range of the accelerometer is 3g and it's sensitivity is 300 mV/g. The maximum bandwidth of this accelerometer is 1.6 kHz and it could be selected using it's capacitive ports. Supply voltage range of accelerometer is between 1.8 to 3.6 V; however, it has been recommended by the producer to be used between 2.6 to 3 V as it's optimum performance range.

A data acquisition device was used to collect the acceleration signals. National Instruments USB-6218 data acquisition was used for this purpose. The device has 32 analog inputs, 2 analog output, 8 digital outputs and 8 digital inputs.Input voltage range of the device is ± 10 V with the maximum of 10.4 V. The device could be

connected to the computer with USB communication as a COM device. Matlab was used to communicate with the pins and collect the data.

3.2. Filter Design

An Infinite Impulse Response (IIR) filter of order three was used while recording the data. IIR filters are also called recursive filters due to the fact that they take the effect of both input and output data [62]. Since IIR filters use feedback or poles they require fewer coefficients. Although this kind of filters are functional in many applications, their tendency to become unstable should always be considered in designing the filter. The general equation of the filter is shown in Equation 3.2

$$H(z) = \frac{b_0 + b_1 Z^{-1} + ... + b_N Z^{-N}}{1 + a_1 Z^{-1} + ... + a_m Z^{-m}} = \frac{\sum_{k=0}^{N} b_k Z^{-k}}{1 + \sum_{k=1}^{M} a_k Z^{-k}} \tag{3.2}$$

where a_k and b_k are filter coefficients. Considering the above formula and taking y(n) as system output and x(n) as system input the IIR filter equation could be written as Equation 3.3 [62]:

$$y(n) = \sum_{k=0}^{\infty} h(k)x(n-k) = \sum_{k=0}^{\infty} b_k x(n-k) - \sum_{k=1}^{M} a_k y(n-k) \tag{3.3}$$

The parameters and equation of designed filter in our experiment is shown in Equation 3.4 (They were defined using Matlab Signal Processing and Communications toolbox):

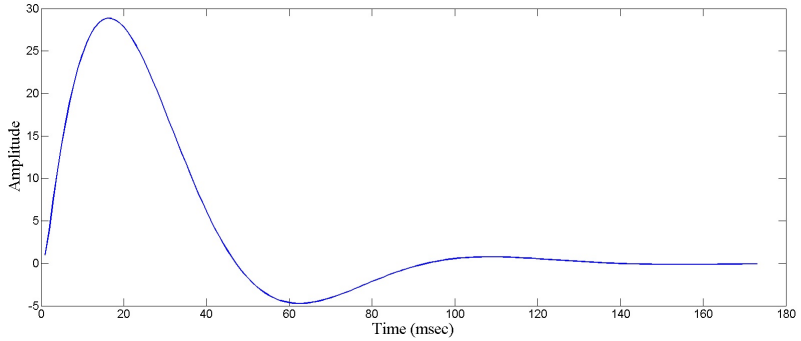

(a) Impulse Response of the IIR filter.

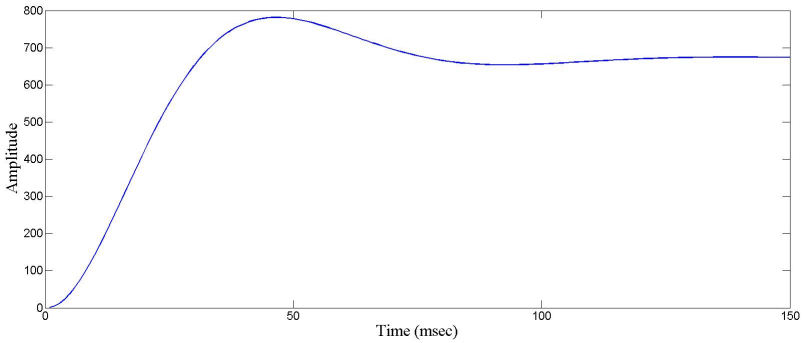

(b) Step Response of the IIR filter.

Figure 3.5. Transient responses of the designed filter.

$$H(z) = \frac{1 + 2Z^{-1} + Z^{-2}}{1 - 1.918Z^{-1} + 0.9244Z^{-2}} \tag{3.4}$$

The transient response of the designed filter (Equation 3.4), including impulse and step responses, are shown in Figure 3.5. The cut-off frequency of the filter is 500 Hz.

3.3. Data Recording Procedure

Data recording of accelerometer and DC motors movement starts at the same time and continues for 5 seconds. The motor stops as it taps (contacts) on the materials.

Contact recognition has been done by using a FSR (Force sensitive resistor) sensor. FSR consist of a conductive polymer, which changes resistance following application of force to its surface. These sensors need simple interfaces and are able to work in variety of environments. Their disadvantage is low accuracy in computing the force which is not important in our study since they are used as touch sensors and not force sensors in data recording experimental setup.

As noted in previous section the four different materials were chosen as experiment samples. The materials are foam (hardness of 10 shore A (Paramonut CO.)), rubber-foam (hardness of 40 shore A (Paramonut CO.)), wood (hardness of 20 HBS) and metal (hardness of 120 HBS) samples. The experimental setup to measure the contact acceleration signals due to tapping on different objects is shown in Figure 3.6. The objects are placed in a position that impact occurs at the linear and constant velocity region. In other words, acceleration of the mechanism is zero at the point of impact.

The results of measured signals for each material is shown in Figure 3.7. As shown in the Figure 3.7 as the velocity of the attack increases the amplitude of the peaks of the transient accelerations response signals also increases. In addition, the difference in characteristics of the signals also is obvious considering the higher frequency of the metal sample acceleration signals (Figure 3.7(d)) and lower frequency of the foam sample (Figure 3.7(a)). Another obvious fact which is seen by looking at the acceleration signals is the decaying criteria of the signals which decreases as samples get harder.

3.4. Signal Modeling and Identification

In order to have a controlled experiment and being able to the change parameters of the signals (if needed), recorded acceleration signals (proposed in Section 3.1) are modeled. In Section 2.2 different models of vibration signals due to tapping have been proposed. In our study we used another modeling to have more control on the

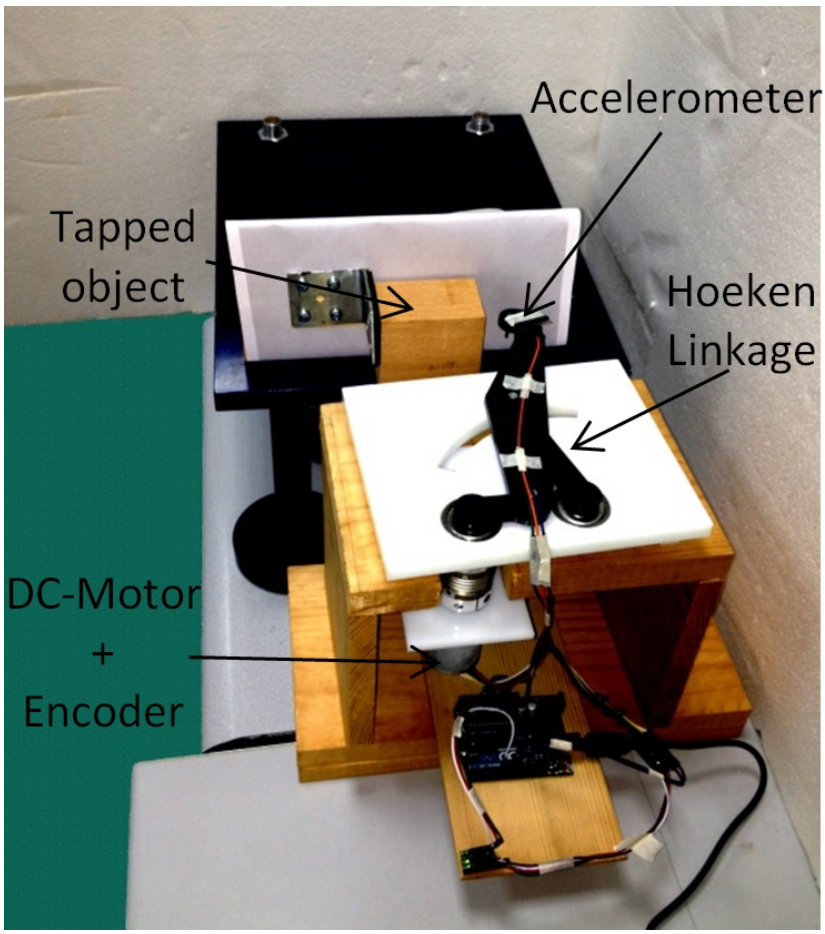

Figure 3.6. Experimental setup for measuring contact acceleration data.

parameters of the signals. The Auto Regressive Moving Average (ARMA) model is the method which is used to model the signals in our study.

ARMA model consist of two different models; AR (Auto regressive) model and MA(moving averages) model. AR model is discribed in Equation 3.5

$$y_{k+1} = \sum_{i=0}^{n} a_i y_{k-i} + \varepsilon_k \tag{3.5}$$

where y(k) is the output, a(i) is the parameter of the model and ε_k is white noise with zero mean and constant variance [63]. MA model could be also described with Equation 3.6

$$y_k = \sum_{i=1}^{n} \theta_i \epsilon_{k-i} + \varepsilon_k \tag{3.6}$$

where θ is the parameter of the model and ε_k is white noise with zero mean and constant variance [62].

Combination of these two models gives the complete for of the ARMA model which the mathematical model of the signal is shown below (Equation3.7).

$$\frac{y(t)}{x(t)} = \frac{\beta_0 + \beta_1 Z^{-1} + ... + \beta_N Z^{-N}}{1 + \alpha_1 Z^{-1} + ... + \alpha_m Z^{-m}} \tag{3.7}$$

where x(t) is input in time domain and y(t) in output in time domain.

Using Matlab Signal Processing and Communications toolbox the parameters of the model was characterized and responses of each model was found. For all models we used ARMA(2,2) modeling. The results of the modelings are presented in Equations 3.8-3.11 respectively for foam, rubber-foam, wood and metal samples.

$$\frac{y(t)}{x(t)} = \frac{1 - 1.83Z^{-1} + 0.8295Z^{-2}}{1 - 0.9247Z^{-1} - 0.07529Z^{-2}} \tag{3.8}$$

$$\frac{y(t)}{x(t)} = \frac{1 + 0.156Z^{-1} + 0.6625Z^{-2}}{1 + 0.9719Z^{-1} - 008704Z^{-2}} \tag{3.9}$$

$$\frac{y(t)}{x(t)} = \frac{1 - 0.2371Z^{-1} - 0.7624Z^{-2}}{1 - 0.06064Z^{-1} - 0.9939Z^{-2}} \tag{3.10}$$

$$\frac{y(t)}{x(t)} = \frac{1 - 0.4167Z^{-1} - 0.5827Z^{-2}}{1 - 0.08098Z^{-1} - 0.0919Z^{-2}} \tag{3.11}$$

The impulse response of the models and the recorded signals for attack velocity of 90 mm/sec are also shown in Figure 3.8.

Further more in order to determine the resemblance of the modeled signals with the recorded signals, cross-correlation of the signals were calculated. Figure 3.9 provides the cross-correlation of each signals with it's model. Also Figure 3.10 shows the cross-correlation of all signals.

As shown in Figure 3.10 the cross-correlation of modeled signable and recorded data overlap. In other words, this shows the resemblance of the modeled data and recorded data. Therefore, these modeled signals could be used for further manipulations.

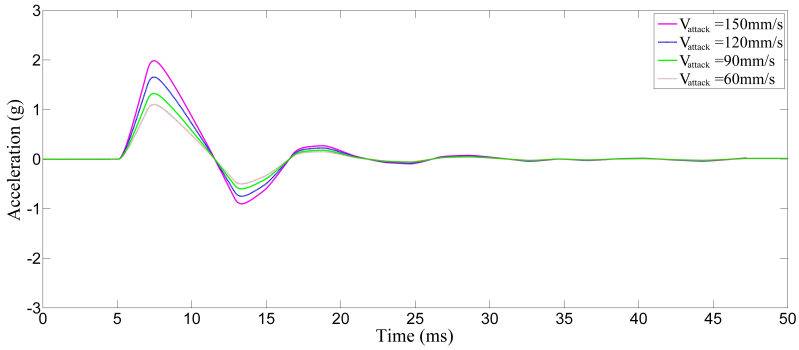

(a) Foam sample.

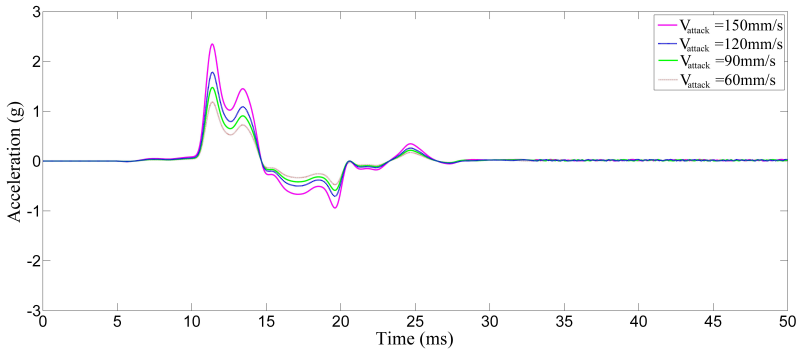

(b) rubber-foam sample.

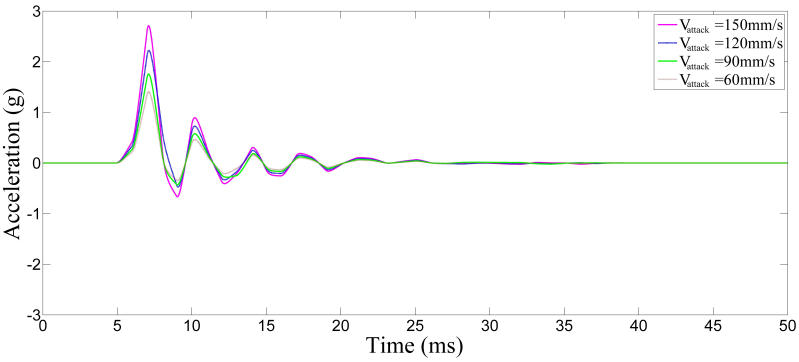

(c) Wood sample.

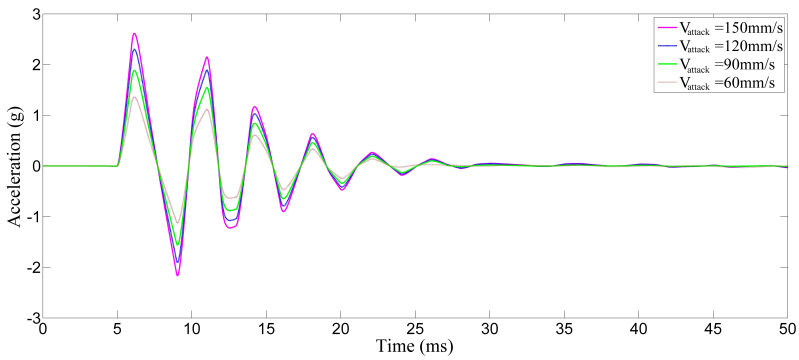

(d) Metal sample.

Figure 3.7. Acceleration response signals recorded due to tapping with experimental setup.

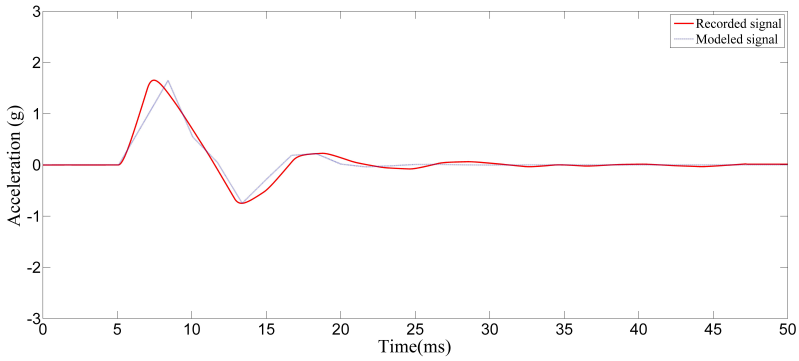

(a) Foam sample.

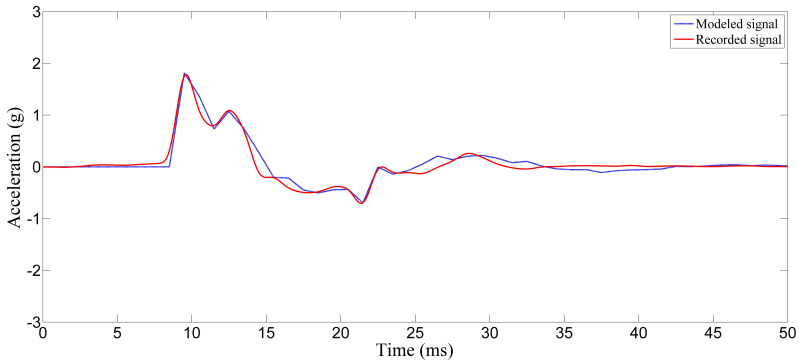

(b) rubber-foam sample.

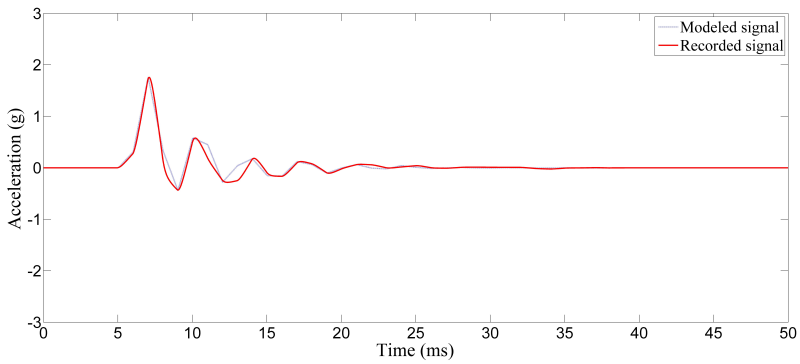

(c) Wood sample.

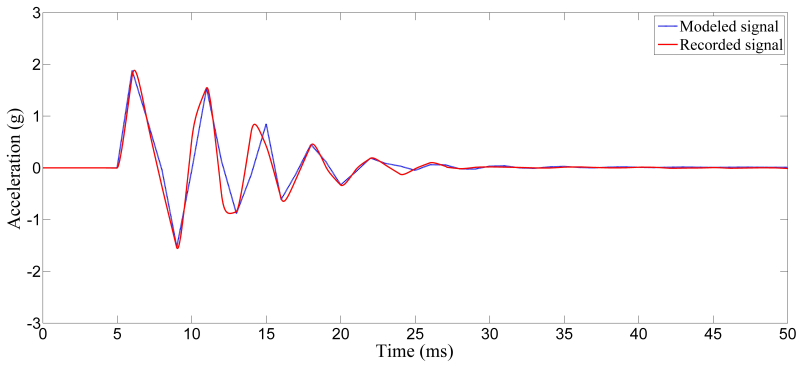

(d) Metal sample.

Figure 3.8. Impulse response of the models and the recorded signals for attack velocity of 90 mm/sec.

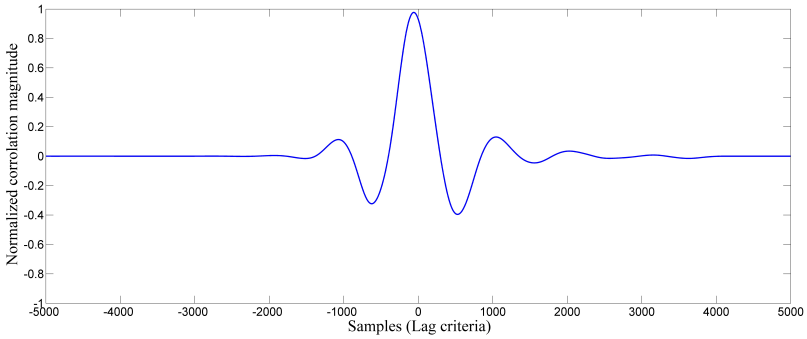

(a) Foam sample.

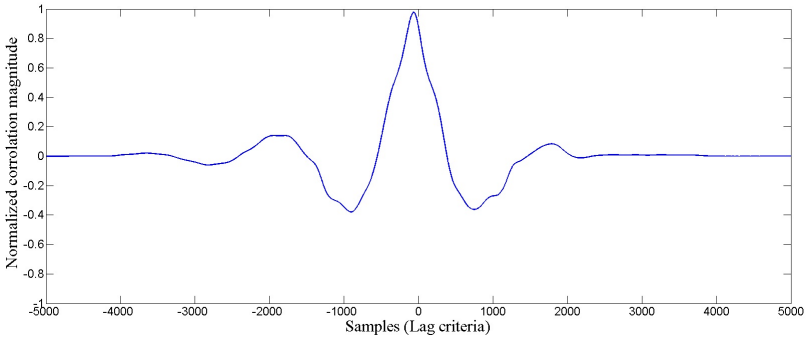

(b) rubber-foam sample.

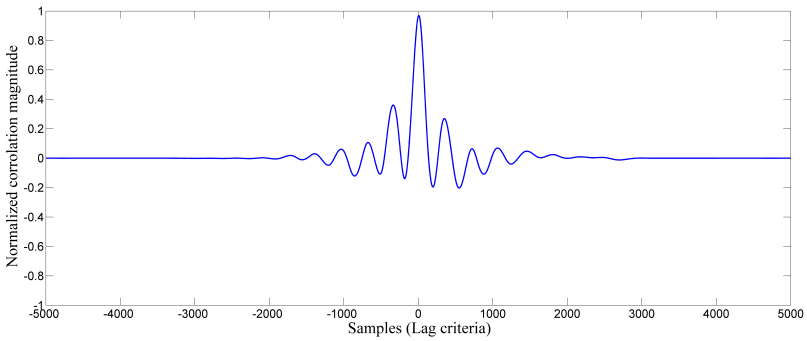

(c) Wood sample.

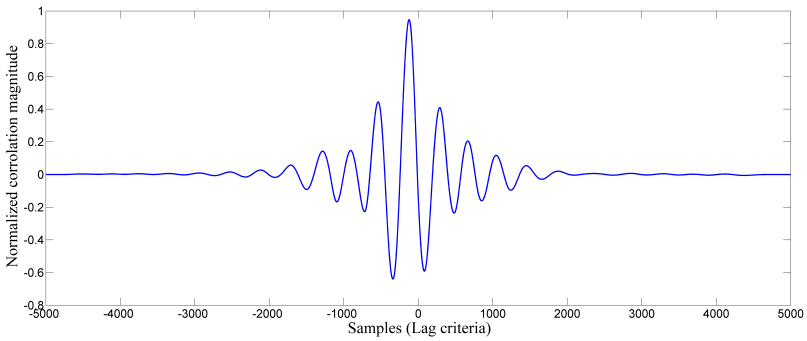

(d) Metal sample.

Figure 3.9. Cross-correlation of the modeled signals with recorded signals.

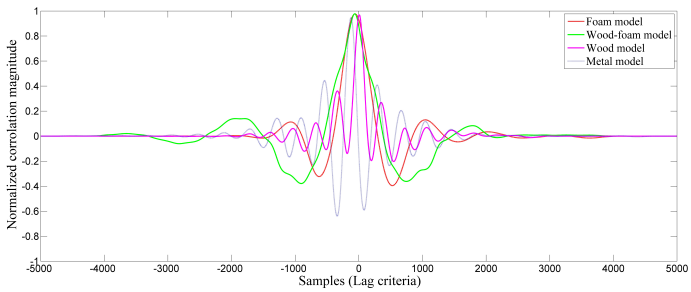

Figure 3.10. Cross-correlation of the all modeled signals.

4. HAPTIC INTERFACE

In order to convey the acceleration response signals to people a haptic interface is needed. The interface should meet variety of requirement and specifications. It should be as simple as possible to be easily used and also should be small enough to fit on clavicle bone without making any difficulty in wearing it. Response of the interface should be fast enough to transmit the desired signal. To satisfy all requirements voice coil linear motor was chosen as haptic interface.

4.1. Voice Coil (Linear Motor)

Voice coil motors are linear actuators which were preliminary used in audio speakers as the source of force to move the panel of speaker, and also were used in disk drive heads as driver of the mechanism. Their special characters includes high power density and high bandwidth. A voice coil is generally an electromagnetic linear actuator which consist of a coils of wire and a magnetic core. Current passes through the coil generates a magnetic field. Force is produced with the reaction of magnetic field of coil and the core [64].

Produced force by Lorents-type actuators (voice coil actuators are Lorents-type actuators) is calculated by Equation 4.1 in which force is linearly proportional to the applied current (Equation 4.1)

$$\overrightarrow{F} = I \times \overrightarrow{B} \tag{4.1}$$

where F is the force(N), I is the current (A) and B is the magnetic field (Tesla).

Considering the structure of the voice coil actuators (Cylindrical wire coils and magnetic core) the force produced by the voice coils are calculated by Equation 4.2

$$F = n\pi dIB\sin\theta_d \tag{4.2}$$

where n is number of coils of wire, d is the diameter of the coil, I is the current flowed in coil and θ_d is the angle between the direction of the current and the magnetic flux. In this study the magnetic core is chosen as the moving part of the actuator. The direction of the movement depends on the direction of the current flux in the coil. Considering the design specification of each voice coils there should be enough voltage applied to the voice coil in order to move the magnetic core with desired amplitude. The velocity and other dynamic characteristics of the movement of the actuator depends on the rate of the current flux inside the coils. Usually current of voice coil is controlled by amplitude of voltage applied to coil.

Using voice coil actuators as tactor (haptic interface) have several advantages as high speed, smooth movements, silence and ease of operation [64]; however, the most advantage of this kind of actuator for our purpose is it's robustness to overloading. In other words, if any force applies to the motor in opposite direction of the movement of the actuator, it simply continues to apply the force and even if the opposite force becomes more than the force applied by the motor it allows itself to be back driven. This property of voice coil actuators ensures it's safety in using it as a device in touch with human body.

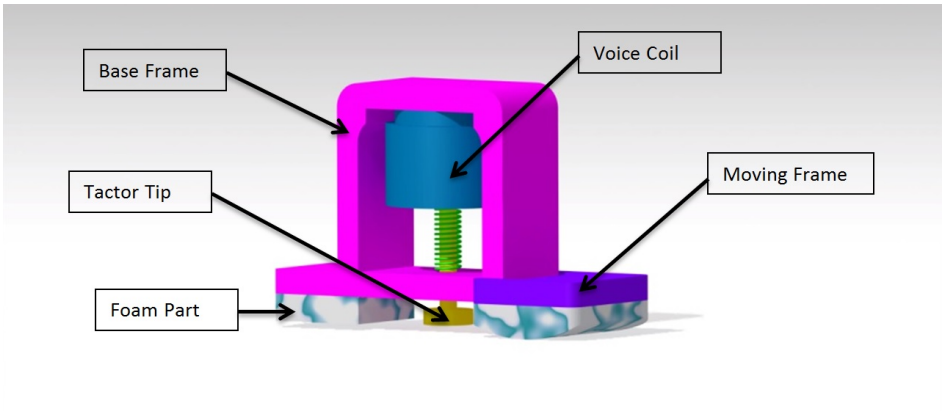

Figure 4.1. Tactor as haptic interface on the shoulder area.

4.2. Actuator Design

In our design we have chosen the magnetic core as the moving part of the voice coil. Since we are going to attach the voice coil on the shoulder area there should be a frame holding the actuator on desired location. Furthermore, other aspects as size and shape of the motor should be considered so the device could be ergonomic. In other words, the designed wearable device shouldn't restrain the normal movement of the body. Taking account of these aspects a tactor has been designed to be attached on the shoulder area. First 3D model of the tactor was designed by CATIA as shown in Figure 4.1.

As seen in Figure 4.1 the base frame part hold the voice coil actuator and also it help the hole device to be not to fall apart in robust conditions. The moving frame also helps the device to be flexible to be compatible for different people. Thin foam parts at the bottom of the frame also neglect the rigid frame irritation of the skin which might happen as the device is attached on the body. The Tactor Tip part is the part of the device which contacts the skin of the user and conveys the desired signals to the user. Moreover, this part will tap on the skin and transmit the acceleration data to the body.

In this study a hand made voice coil motor had been designed (Figure 4.2). The

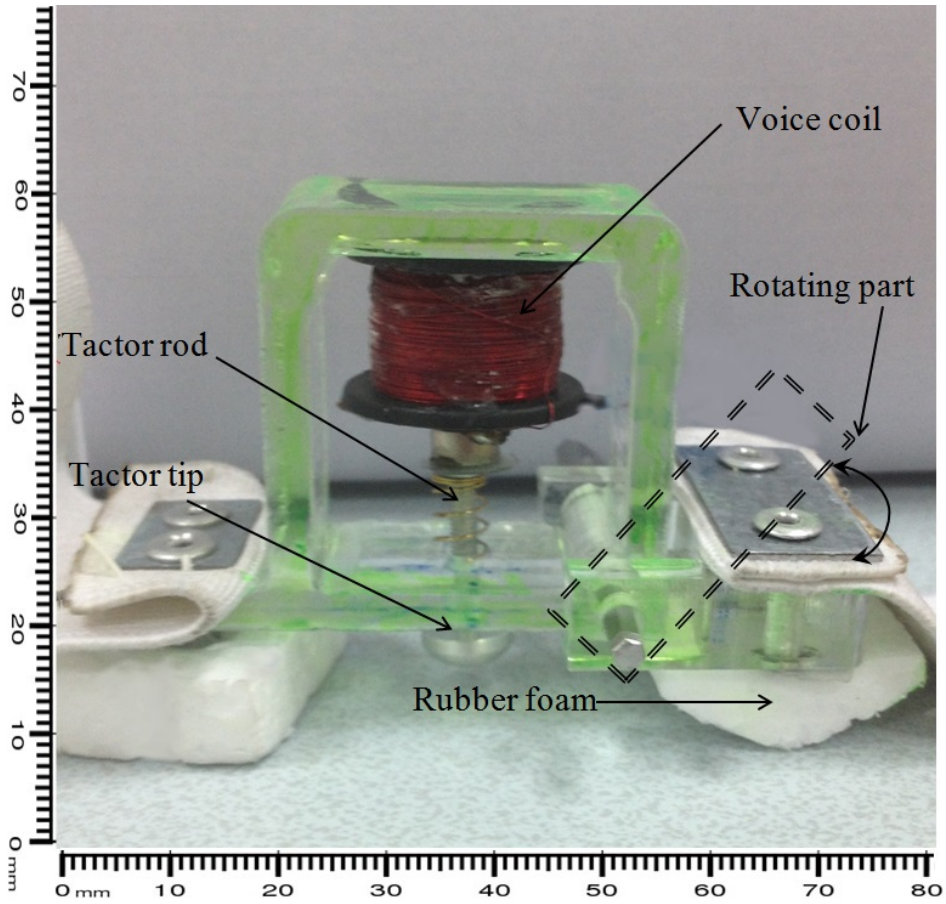

Figure 4.2. Hand-made Tactor.

outside diameter of the coil is 22 mm and and the inside diameter is 5 mm. Wires used in the coil are 0.1 mm shielded wires wrapped around a plastic cage for 3400 rounds. The wrapping has been done by a special wire wrapping machine to be constant and ordered. The plastic cage is made by plexiglass and the Tactor-Tip was made from Aluminium. The core of the voice coil is also a 3 mm cylindrical magnet with magnetic field of 340 mT. Using Equation 4.2 the voice coil generates approximately 1.7 N continuous force.

Different studies has been done on finding an appropriate model for a voice coil linear motor. One of the first and popular models that has been used for linear motors is a model which describes it as a third order damping system [65]. The model's transfer function is shown below:

$$G(s) = \frac{U(s)}{X(s)} = \frac{1}{\frac{mL}{B_gL}S^2 + \frac{mR}{B_gL}S + B_gL} \cdot \frac{1}{S} \tag{4.3}$$

Neglecting the inductance (L) from the model which normally is so small results in following model:

$$G(s) = \frac{U(s)}{X(s)} = \frac{1}{\frac{mR}{B_gL}S^2 + B_gLS + \frac{kR}{B_gL}} \tag{4.4}$$

In Equation 4.4 U is the input voltage, X is the position of the moving part of the voice coil motor, m is the mass of the moving part, B_gL is force constant of the motor and k is the coefficient of the spring if there is one in the motor.

Considering the model described in Equation 4.4 and the parameters of designed voice coil in the study (m = 80 gr , R = 14 Ω , B_gL = 4 N/amp , k = 41 N/m), our systems model could be represented as below:

$$G(s) = \frac{U(s)}{X(s)} = \frac{1}{0.28S^2 + 4S + 143.5} \tag{4.5}$$

Using the model shown in 4.5 the system's transient responses (to step and impulse inputs) are shown in Figures 4.3.

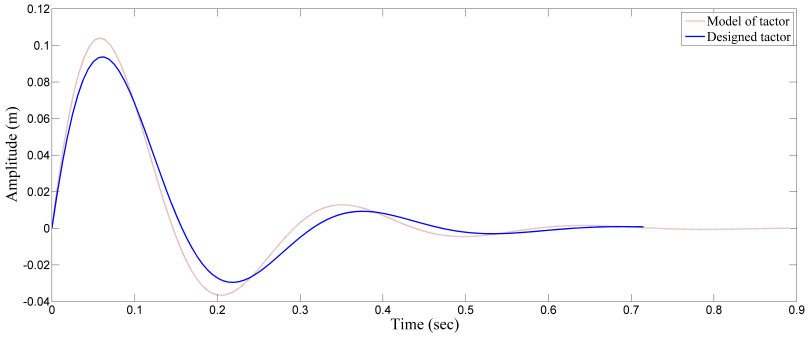

(a) Impulse response of both model and designed voice coil motor.

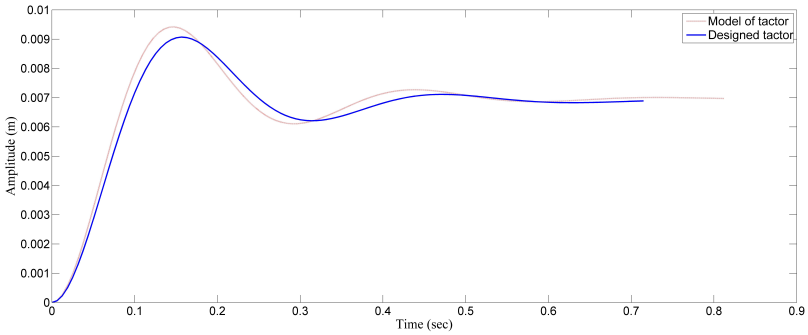

(b) Step response of both model and designed voice coil motor.

Figure 4.3. Transient response of both model and designed voice coil motor

Rise-time of the model is 0.0595 sec and the settling-time is 0.4940 sec. Transient response of the designed voice coil is also shown in Figure 4.3. Rise-time of the designed voice coil is 0.0651 sec and the settling-time is 0.5178 sec.

Figure 4.4 shows the FFT of the input (a sine wave with frequency of 5 Hz) and output signals to the voice coil motor's model. As shown in the noted Figure the model contains the important criteria (main frequency) of the input signal. Figure 4.5 also shown the impulse response of the designed voice coil.

In order to verify the function of the voice coil motor the output of the motor to the same sinusoidal input signal (Voltage) has been measured using a Polytec's PDV-100 Portable Digital Vibrometer. Using this system the vibration (velocity) of the tactor head was measured by importing the sinusoidal signal as voltage. The FFT of the output is shown in Figure 4.6.

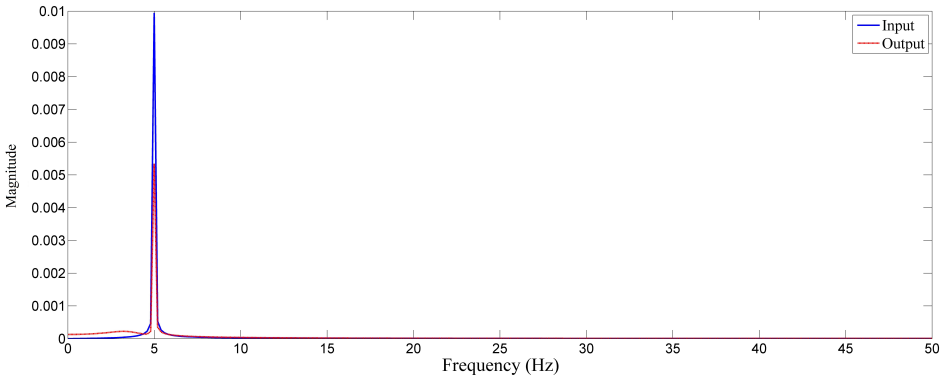

Figure 4.4. FFT of the input and output signals to the voice coil motor's model.

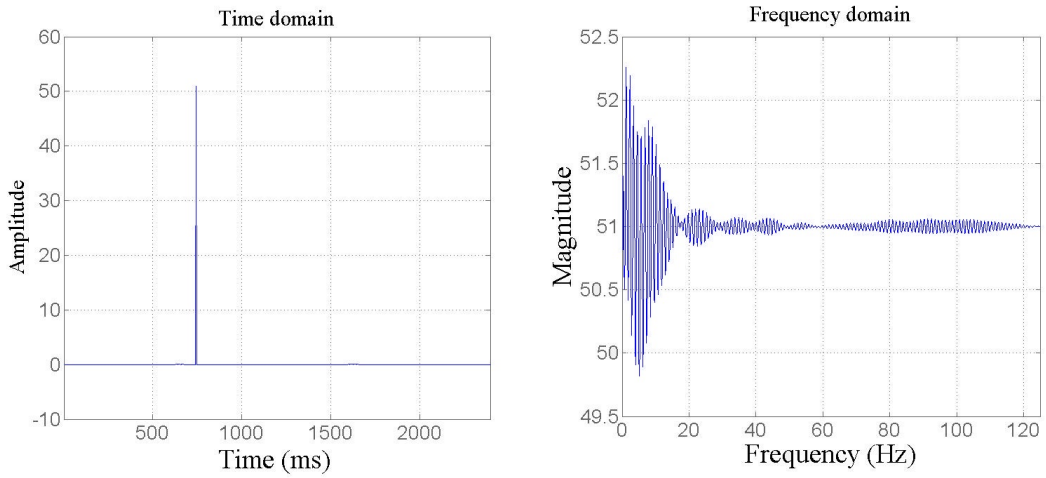

Figure 4.5. Impulse response of the designed voice coil.

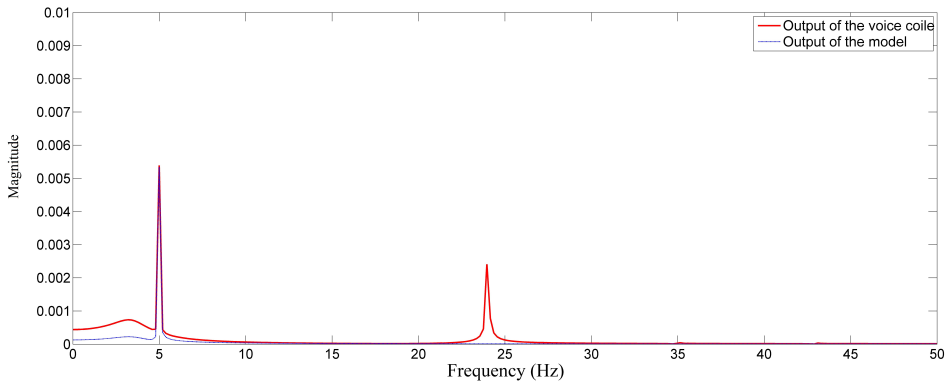

Figure 4.6. FFT output of the model and output of voice coil motor to the same input sinusoidal signal.

As shown in Figure 4.6 there are other frequencies shown in the measured output FFT of the voice coil motor. As described in [66, 67] this error in due to hysteresis phenomenal in voice coil motors. Defining this phenomenon in the model of the motor needs a higher order model like the model used in [68, 69] in which 10 and 12 order models have been used to provide sufficient model of the system. However such model could describe the system with details, for our use we do not need that much of detail due to the range of the sensitivity of the clavicle bone.

5. REAL TIME IDENTIFICATION

In order to make the whole system to work in real-time, acceleration response signals (Due to tapping on different materials) have to be identified in real-time procedure. First criteria of the signals which could be used as discrimination tool are the frequency and damping of the signals. As shown in Figure 3.7 as the material get harder the frequency of the acceleration response signals are getting more. Using logarithmic decrement damping ratio of materials are $\zeta_{foam} = 0.383$, $\zeta_{wood} = 0.140$, $\zeta_{metal} = 0.067$. More over the settling time of the softer materials are more than hard er ones. This criteria of the signals has been used as the first criteria of identification; and experimental results of using this method has been printed in [70]. A time history of the real-time experiment using this method of identification is shown in Figure 5.1. The whole procedure, from the time that the tapping occurred to the end of feedback given by the interface, takes around 120 msec. The delay between the feedback and the actual contact is about 60 msec.

According to Okamoto *et al.* [71] less than a 40 msec delay in haptic interface devices is not perceivable. As shown in Figure 5.1 there is a 60 msec delay by using the identification method described above. However the preliminary experiments didn't show any perceivable delay, further research has been done to find an identification method which could lower the delay time to be less than 40 msec.

Looking at Figure 3.7 clears the fact that rate of the change of the acceleration response signals are different for different materials. Exploiting this fact reveals a the second method to identify the hardness based on the acceleration response signals recorded by tapping on different materials. In order to find the capability of this method an interface has been designed using MATLAB Graphical User Interfaces (GUI). Using this interface and the same experimental setup described in 3.1 by tapping on different materials the errors of the system in correct identifying has been measured. The

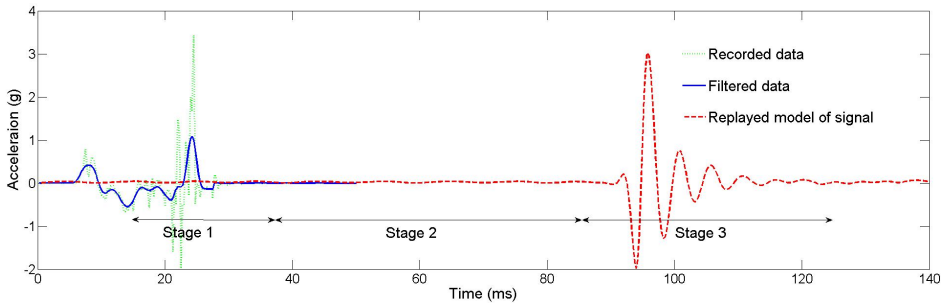

Figure 5.1. Real time experiment's time history: At stage one, the acceleration response is captured and filtered. At stage two, the processor defines the tapped object as hard or soft object and selects the desired signal based on the impact velocity. At stage three, the haptic interface applies the appropriate signal on the clavicle bone.

interface is shown in Figure 5.2.

Using the second method of identification - as the first method - a time history of the real time experiment has been recorded. The time history related to the second method of identification is shown in the Figure 5.3. As it is demonstrated in the Figure 5.3 it takes around less than 30 msec to identify and start to play the appropriate signal after the acceleration response signal occurs due to tapping on an object.

As shown in Figure 5.2, five different hardness rates (using one to five respectively as soft to hard) were selected as hardness scale to chosen using the second method of the identification. Using this interface the second method of identification has been experimented to find how accurate could this method be considering the correct identification. Ten trials has been done on each material. Based on the number between one to five (Representing respectively from soft to hard) the average estimated hardness selected for material were 1.1, 2.1, 3.2 and 4.5 for respectively foam, rubber-foam, wood and metal samples. Considering scale one for foam, two for rubber-foam, three for wood and four and five for metal, the error in identifying the hardness was less than 5 percent. All the processing of real-time identification has been done by Arduino uno Processors.

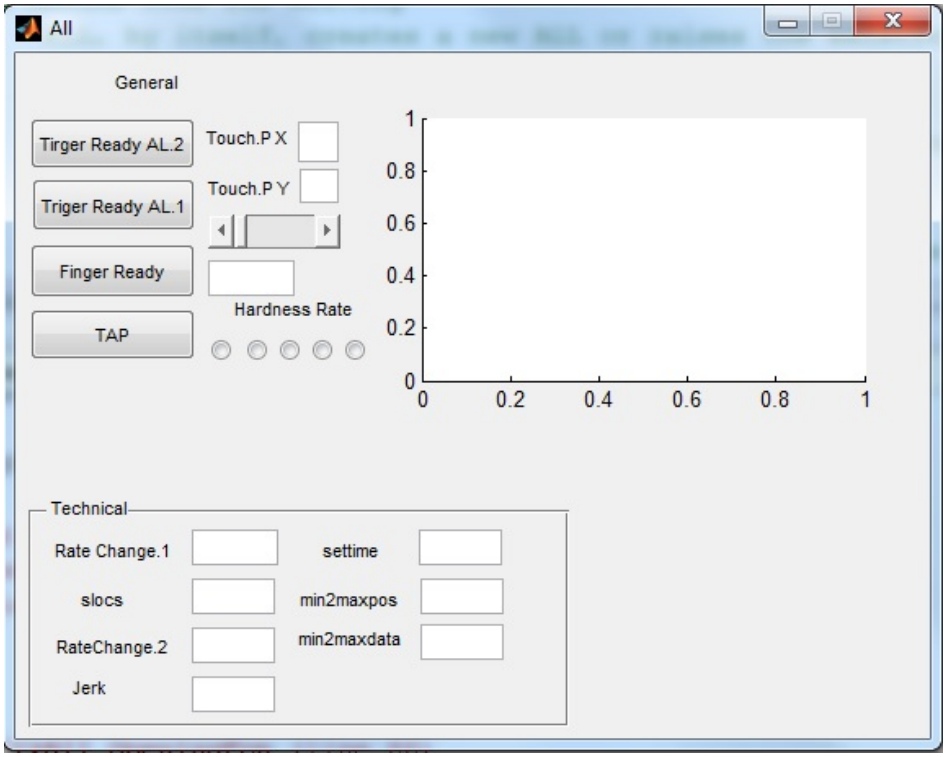

Figure 5.2. Identification interface designed by MATLAB Graphical User Interfaces (GUI).

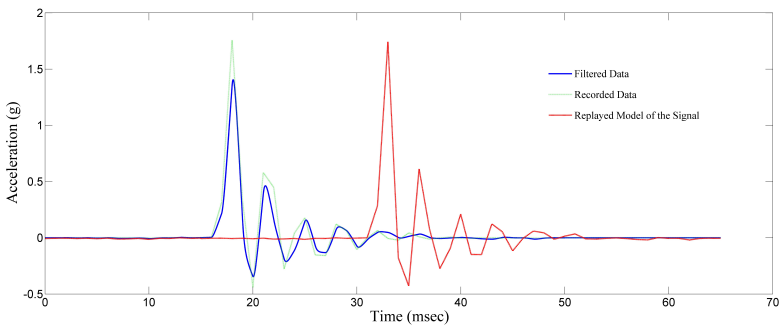

Figure 5.3. Real time experiment's time history using the second method of identification.

6. PSYCHOPHYSICAL EVALUATION

The design and evaluation of the haptic device and the desired real-time procedure has been discussed in the previous chapters; However, in order to figure out the functionality of the whole system and understand whether the desired sensation has been properly perceived by users, a set of human subject study has been conducted. All the experiments and subject tests have been approved by the Institutional Review Board (INAREK) of Bogazici University and performed at the Haptics and Robotics Laboratory of Bogazici University.

As noted above the aim of the human subject test is to figure out if the designed tactor (Section 4.1) and used methods (Chapter 5) are practically useful to convey the hardness sensation in real-time. Therefore, firstly it has to be understood weather the users of the tactor could discriminate the hardness feeling of different materials and secondly if the whole system confronts with a delay which could make problem in real-time use.

In order to figure out the ability of the users to discriminate the hardness of different materials, a magnitude estimation test, using four acceleration signals described in Section 3, has been developed. Also testing the real-time capability of the system has been done using an experimental setup in which subjects control a mechanism (by moving their finger which was attached to a controlling device designed for this study) to tap on different materials; as the mechanism taps on different materials the tactor plays the appropriate signal on the clavicle bone of the subjects and they were asked to stop their as they feel tapping on their clavicle bone. The real-time capability of the system was measured through the error which users make in stopping their finger (More description in Section 6.2).

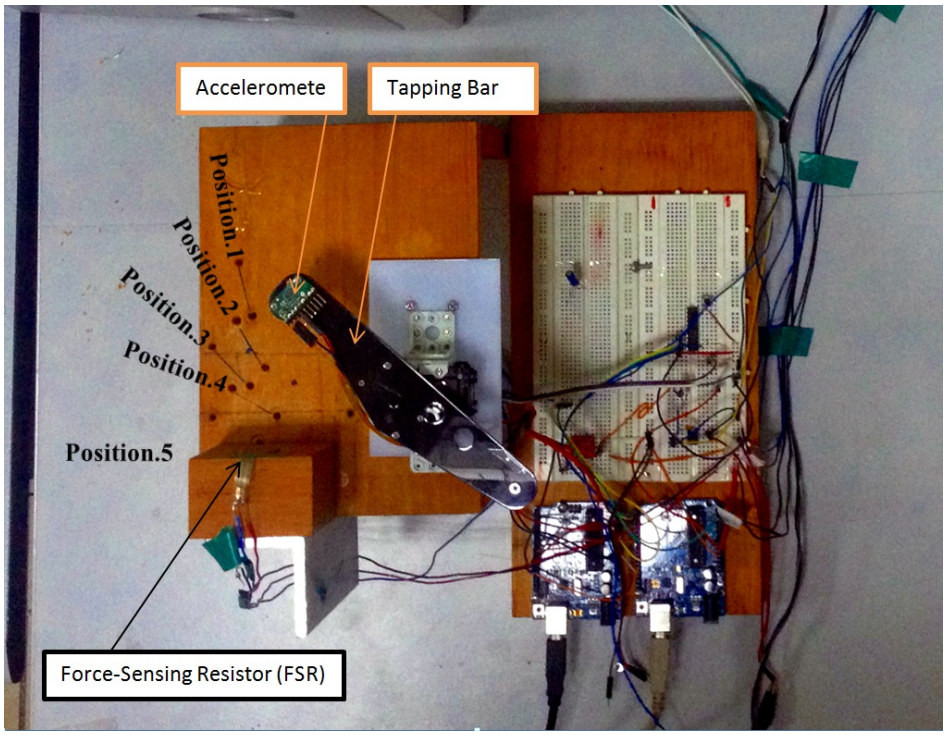

Figure 6.1. Tapping mechanism.

6.1. Experimental Setup

In order to perform human subject tests, an experimental setup has been developed. The setup contains electrical and mechanical parts to fulfill the required results from the tests. Following subsections describe different parts of the experimental setup.

6.1.1. Mechanical part

As describe in the beginig of this Chapter, the experimental setup contains a mechanism to tap on different materials. This mechanism was built as representation of a prosthetic hand in which also no sensation is felt by interacting with environment. As shown in Figure 6.1 a tapping bar is used in the mechanism to tap on different materials. The mechanism is driven with a Dynamixel AX-12 servo motor. An accelerometer is attached on the bar to capture the acceleration response signals.

In the human-subject test, the tapping bar is remotely controlled by the tip

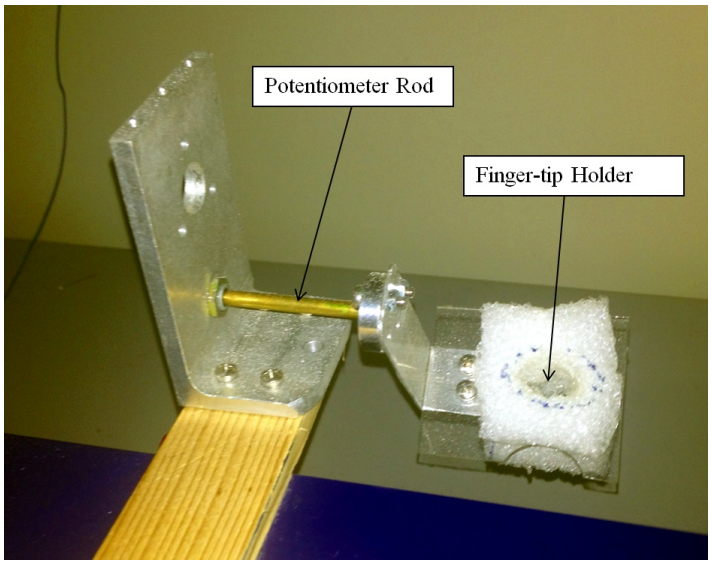

Figure 6.2. Designed device for tracking the finger-tip position of the subjects in human subject experiments.

of the finger of the subjects using a device shown in Figure 6.2. As shown in the Figure 6.2, the device contains a place to place the finger-tip of the subjects. As the subjects try to revolve their finger using a rod (Which is attached to a potentiometer) the position of the potentiometer changes. Using the data coming from potentiometer (with the resolution of 1024 counts per 240 degree), actuator of the tapping mechanism (Dynamixel AX-12 servo motor) tracks the position of the finger-tip of the users (Figure 6.1).

As shown in Figure 6.3 the rotation angle of the finger (As they move their fingers) is mapped to rotation degree of the motor used to revolve the tapping bar. Using this mechanism subjects tap on materials in a remote place without filling the actual tap sensation on their finger.

6.1.2. Electrical part

In order to control the motors (tapping mechanism motor and voice coil motor of tactor), capture the acceleration signals, filtering and identification of the system, three Atmega 328 microprocessors (on Arduino UNO cards), one LF-411 op-amp amplifier

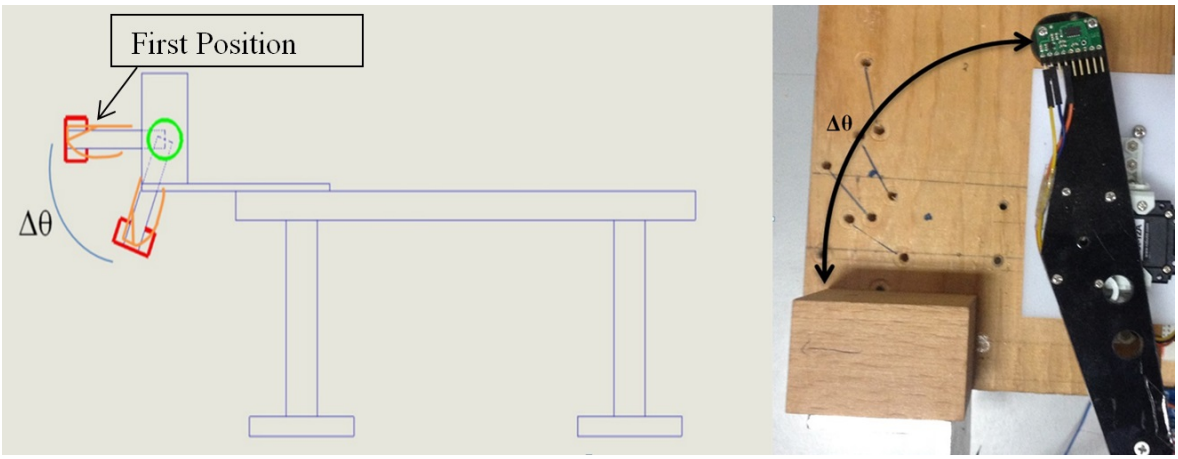

Figure 6.3. Position of the finger tip is tracked by a potentiometer.

, one MCP4725 Digital to Analog Converter (DAC) and one 74LS241 chip have been used in experimental setup. Three Arduino Uno (Atmega 328 Processor) in the whole experimental setup; one for tracking the finger-tip position with a potentiometer (6.1.1) and controlling the servo motor (Dynamixel AX-12) of the tapping mechanism, one for recording the acceleration data, identification and sending the appropriate signal to the voice coil and another one to record data imported by the users with a 4×4 keypad.

Since Arduino Uno can't write analog signals a MCP4725 Digital to Analog Converter (DAC) chip has been used to send analog voltage signals to voice coil motor. The I2C communication protocol has been used to communicate with MCP4725 DAC with Arduino Uno. Also an LF-411 op-amp has been used to amplify the signals sent from Arduino Uno to the voice coil. Since Dynamixel AX-12 communication is Half Duplex UART-TTL and a three-state buffer is needed to make this communication available, a 74LS241 chip is used to overcome this problem. Communication between Arduino and 74LS241 chip is done using serial communication. Further data of chips used in experimental setup could be found in Appendix B.

6.2. Experimental Procedure

In order to evaluate the performance of the designed sensory feedback system in Real-time a human subject test has been performed. Ten subjects pariticipated the

Figure 6.4. Tactor on the body.

test. People who have joined to the test were between twenty two (22) to thirty one (31) years old including nine men and one women.

As described in Section 1.3 the main purpose of this thesis was to fed the contact sensory feedback on the clavicle bone (Figure 1.2). In order to achieve this goal the tactor (Section 4.1) has to be attached on the shoulder area how that the tactor tip (Figure 4.2) would be on the clavicle bone. Tactor is attached on the body using rubber straps which could be adjusted for each subject(Figure 6.4). Before starting the test, tactor was fixed on each subject using the straps.

Four different sample materials and their signals (Described in Chapter 3) are used in human subject test. After fixing the tactor on the body of each subjects they were asked to sit on a chair comfortably (Figure 6.5). Some initial information about the test has been described to subjects before starting the test; however, they were not informed about the details in order to avoid any pre-defined judgments. The human subject test contains three stages as Training, Magnitude estimation and Position control. Theses stages are described in following subsections.

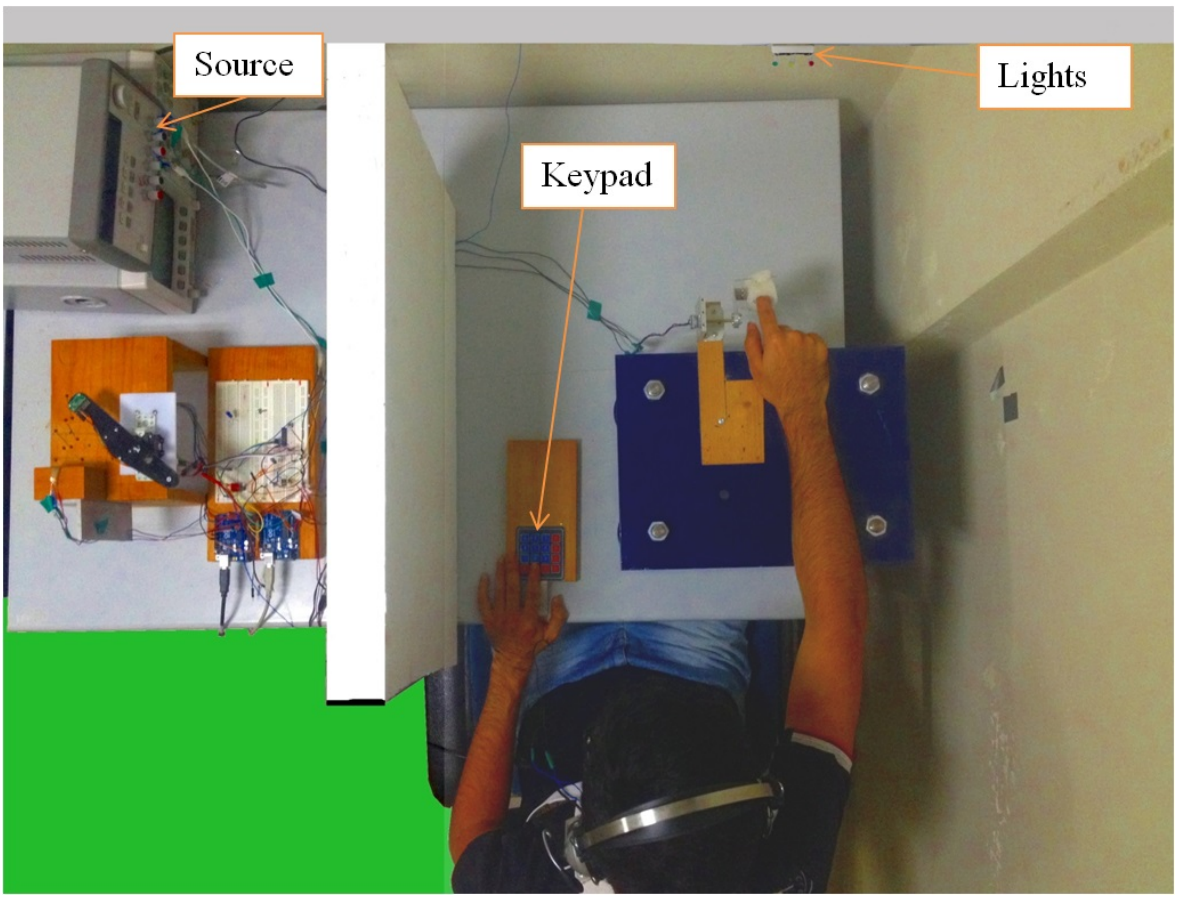

Figure 6.5. Experimental setup

6.2.1. Training

As the first stage of the human subject test the four signals randomly were played to each subject to make them familiar with the intensity of the signals. There was no questions asked to the subjects at this stage. Signals were randomly played for each subject with a time delay of five seconds between each signal.

6.2.2. Magnitude estimation

The second stage of the test starts after the training stage. The purpose of the second stage was to understand the perceived magnitude of the hardness of each of the four signals. In order to achieve this aim, a magnitude estimation test [72–74] has been conducted. The method of magnitude estimation is a psychophysical method in which the numerical estimation of sensation magnitude is measured through series of stimuli with variety of intensity [75]. The validity of the magnitude estimation results depends on demonstration of the fact that the measured numbers are in relation with known measurements. The hardness of the sample materials (and their acceleration signals) are known as soft to hard relatively for foam, rubber-foam, wood and metal.

As described above in the second stage the hardness magnitude is going to be estimated by the users. In this stage each signal is played for subjects for three times randomly resulting in totally twelve signal played on each subject. After playing each signal on participants they were asked to estimate the hardness sense of the tap (played by tactor on their clavicle bone) felt on their clavicle bone as a number between zero to nine; considering zero as the softest felt sensation and nine as the hardest one. The subjects indicated the numbers using a keypad shown in Figure 6.5. Numbers were collected automatically for each subject and stored for further analysis. Next signal was played five seconds after the user entered the magnitude related to previous signal. Throughout the whole experiment participants wore a headphone (playing white-noise)to avoid sound feedback which could affect the results.

6.2.3. Position control

The third stage of the experiment starts five minutes after finishing the second stage. In this five minutes subjects were asked to sit relaxed while the operator make the system ready for the third stage. The purpose of the third stage was to identify the role of contact sensory feedback in controlling the robotic prosthetic devices. Furthermore, this stage was performed to understand weather this sort of feedback could help users of robotic prosthesis in controlling the position of their robotic fingers. Since contact information is the first tactile information which is received in any interaction with our environment, this sensation could be helpful for users of robotic prosthesis to realize interactions with physical objects and improve their control on their prosthesis. If the sensory feedback system doesn't work fast enough, the delay between touching an object and feeling the sense of touch could make variety of problems in controlling the robotic prosthesis such as braking or falling the touched objects. Further more severe understanding of the materials hardness could be also beneficial in grasping function and could decrease the error in choosing the velocity of grasp in re-pushing the object [76]. Experimental procedure in stage three of the experiment is repeated two times with two different feedback conditions; without visual feedback and with visual feedback.

Stage three of the human subject test starts with asking participants to put their fingers in the finger-tip holder as shown in Figure 6.2. As described in Section 6.1 as they move their finger, the tapping mechanism moves and imitates the tapping function with a robotic prosthetic device. In this experiment four materials were randomly placed in five different positions in front of the tapping mechanism (Figure 6.1). As the subjects move their fingers the tapping mechanism would tap on different sample materials placed in different positions. Position of sample materials were also chosen randomly. Before starting the experiments users were asked to move their finger, attached to the finger-tip holder, and watch to the synchronized free move of the tapping mechanism. This has been done to make them familiar with the experimental

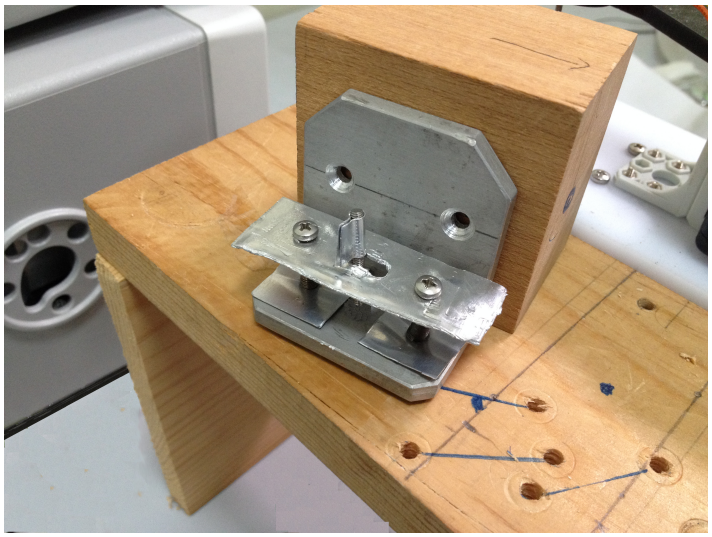

Figure 6.6. Fast clamping mechanism to fix the position of the sample materials in different positions.

setup.

At this stage a barrier was placed between subjects and the tapping mechanism and a headphone was worn by subjects throughout the whole experiment so they wouldn't have any visual or sound feedback. Participants were asked to move their finger , attached to the finger-tip holder, and stop when ever they felt the sensation given by the tactor on their clavicle bone. After each try materials were placed randomly in different positions (Figure 6.1). Subjects were informed to start moving their finger with a green light located in front of them as shown in Figure 6.5. At each trial, after they stop, they were asked to remain at the stopped position until a red light in front of them flashes so they could go back to the first position (Figure 6.3) and start the next trial. The red light flashes manually by the operator after placing another sample material (Or the same one dependent to the random selection) in another position. In order to change the position of the materials and fix them in desired positions quickly a clamping mechanism was designed as shown in Figure 6.6.

As the tapping mechanism (Figure 6.1) taps a random sample material in a random position the tactor plays the appropriate signal on the clavicle bone of the

subjects; and they were asked to stop their finger as they feel the tap on their clavicle bone. The error between the user's finger-tip position when the tapping occurs (by the tapping mechanism) and the position in which participants stop considered to be the positioning error. A Force Resistive Sensor (FSR) is used to sense the tapping action of the mechanism . Furthermore, for a person, natural sensory system let him/her to control the position of the finger immediately after touching an object. If the sensory feedback system in our study works well there should be a small error between the position in which the tapping occurs and the position in which the users stop. However as described in Section 5 the delay of the system is less than thirty msec, the real perception and functionality of the system could be understand performing stage three of the human subject test. Every position and each sample materials were used for three times randomly resulting in sixty trials for each subject.

As noted above this stage of the experimental setup is done for two conditions; without visual feedback and with visual feedback. The second part of the third stage of the human subject test includes the same procedure with visual feedback. At this part participants were asked asked to go through the same procedure in the first part of the third stage by looking at the tapping mechanism. The purpose of this part of the experiment was to measure the position error which occurs while performing the same experiment with visual feedback. At this stage the tapping mechanism was not included in the experiment and steel the headphone was worn by participants.

6.3. Results and Discussion

As noted in Sections 6.2 after the training stage of the human subject test, at the second stage a magnitude estimation has been done to measure the perceived magnitude of the hardness of each acceleration response signal. Data of this stage of the experiment has been collected and saved automatically. After collecting the data for all 10 participants in the human subject test their data has been imported to SPSS software for further statistical analysis. Please note that harness scales of

softer materials (foam and rubber foam samples) could not be interpreted in the scale of harder materials (wood and metal samples).

As shown in Figure 6.7 foam, rubber-foam, wood and metal estimated from soft to hard by the participants. Same order of the softness was also determined for signals before human subject experiment (Section 6.2). Statistical information for results of magnitude estimation are shown in Table 6.1. A pair-wise t-test was performed on results of magnitude estimation to see wether estimated hardness magnitudes for each signal are significantly different or not. Taking α=0.05, the t-test results showed that each pair of the signals are significantly different with each other. Results of this stage of the experiment shows acceleration signals played by the tactor are completely distinguishable from each other considering their felt sense of hardness. This approves the ability of the designed tactor to convey distinguishable hardness feeling to the users.

The position errors are measured in degrees; moreover position error is the angle (In degrees) which the user's finger move after the tap occurs by the tapping mechanism. As demonstrated in Figure 6.8 position Error described as $\delta\theta$, the angle which is past after the tapping bar contacts the sample material.

Table 6.1. Statistical Information for magnitude estimation stage (Stage two) of human subject test.

Material/Statistical Information	Mean	Range	Standard Deviation
Foam	1.9	1	0.31618
Rubber Foam	4.1653	2	0.65131
Wood	6.5320	2.66	0.77179
Metal	8.599	1.99	0.60337

As described in Section 6.2 position errors were measured in two conditions, without visual and with visual feedback (no haptic feedback). One-way analysis of

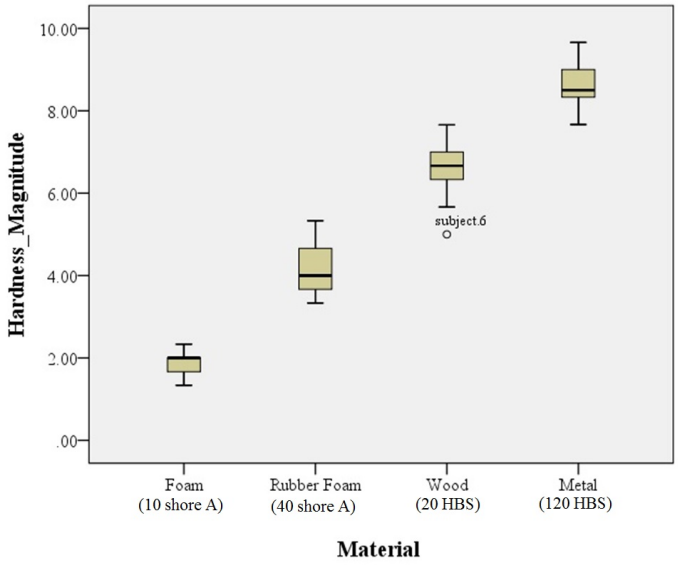

Figure 6.7. Magnitude estimation of hardness for each material measured from human subject test.

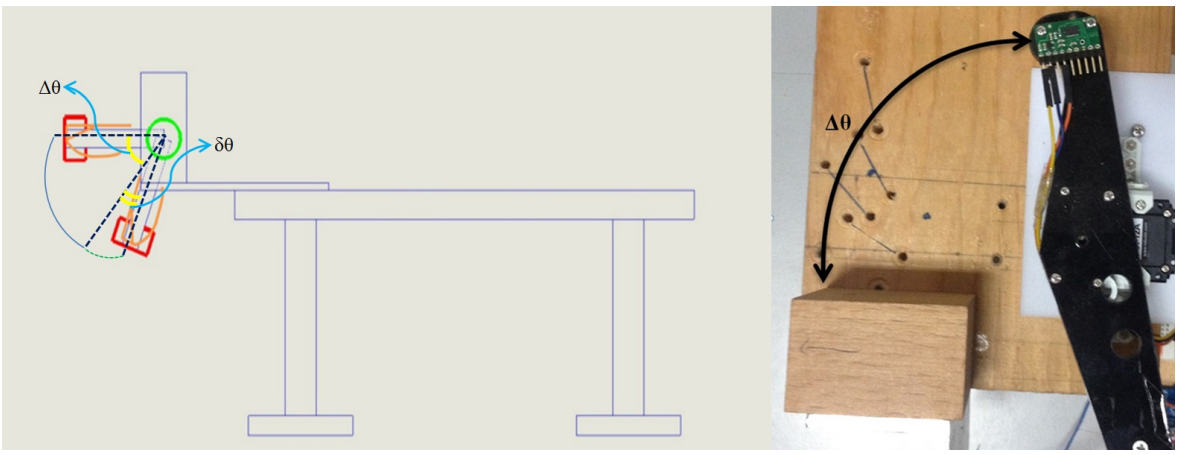

Figure 6.8. Position Error measured at stage three of the human subject test.

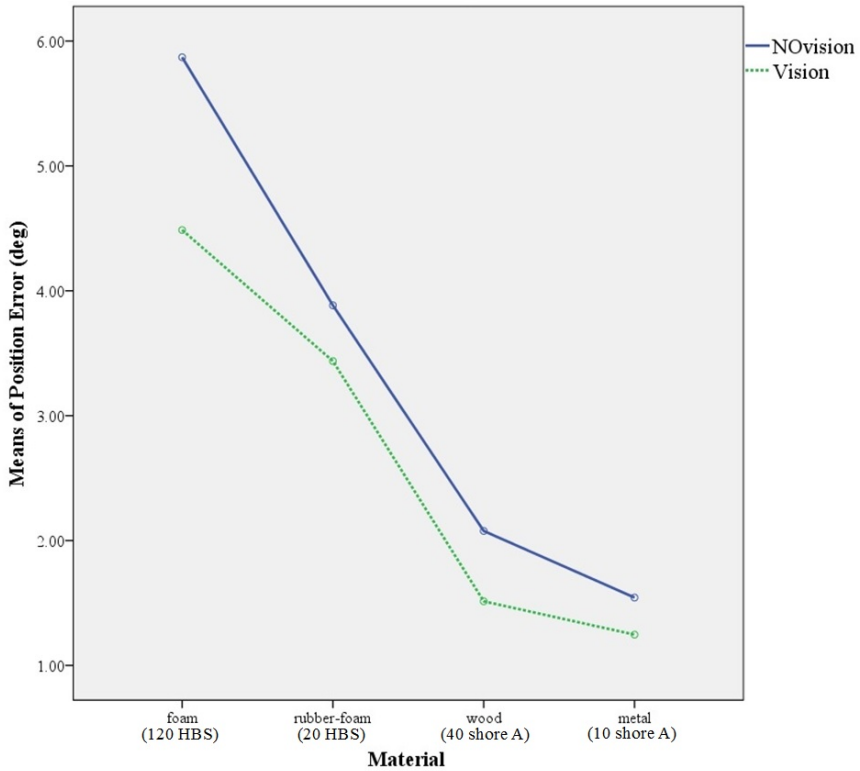

Figure 6.9. Position Error considering the Material for two Vision conditions (without visual and with visual feedback)of the human subject test.

variance (ANOVA) [47, 77] was applied for two factors of Vision (without visual and with visual feedback)and Material (Four sample materials) to realize their significance in the experiment. Choosing $\boldsymbol{p}$ =0.001 demonstrated the fact that both Material and Vision are significant in the results. As shown in Figure 6.9 for each Material the position error is smaller in the condition that experiment has been done with visual feedback. This is also obvious that as materials get harder the position errors decreases. It is also seen at Figure 6.10 that foe two condition of Vision (without visual and with visual feedback (no haptic feedback)), the position error for each material is less for the condition with visual feedback.

Another One-way ANOVA,$\boldsymbol{p}$ =0.001, done for two factors of Material (Four sample materials) and Position (Five different fixing positions to fix the sample materials) showed the fact that fixing position of the sample materials did not have a significant effect on the positions error (Figure 6.11).

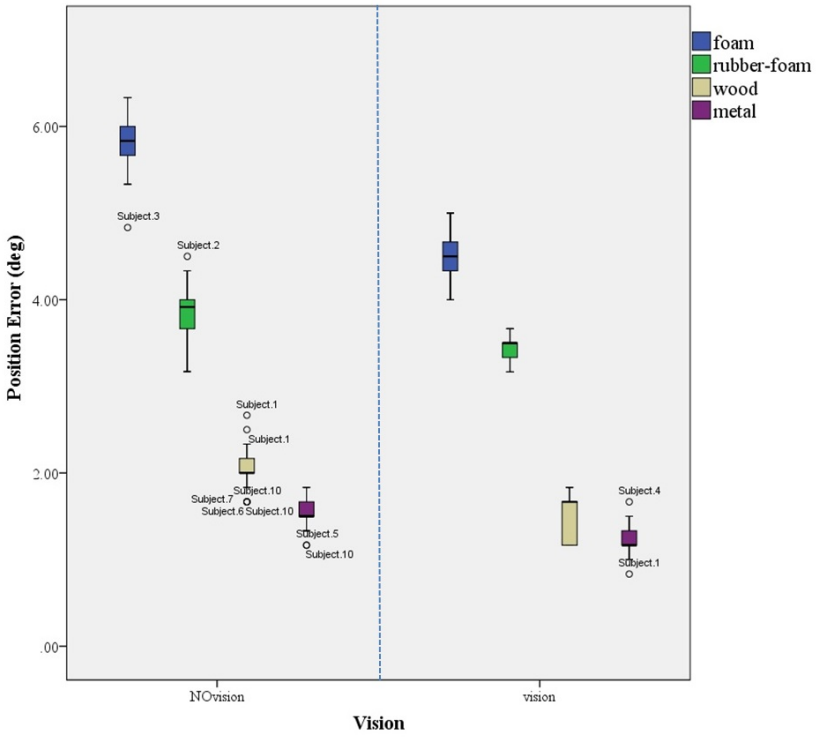

Figure 6.10. Position error considering the material for two vision condition of human subject test.

Generally looking at the results of the third stage of the human subject experiment, shows that although errors in case of visual feedback are less, the difference between the two cases aren't that much (Figure 6.12). Considering average index finger size to be ninety mm [78], one degree of revolution of the finger results in 1.57 mm of finger-tip movement. Since the maximum position error difference between the visual and no visual feedback is 1.4 degrees, the maximum finger-tip position difference between the this two condition becomes 2.2 mm. It is also seen that errors in stage three are lower for harder samples. Since the touch sensor on the softer samples dents inside and it cause sensors to detect touch with delay; this could be the reason for more error of softer samples.

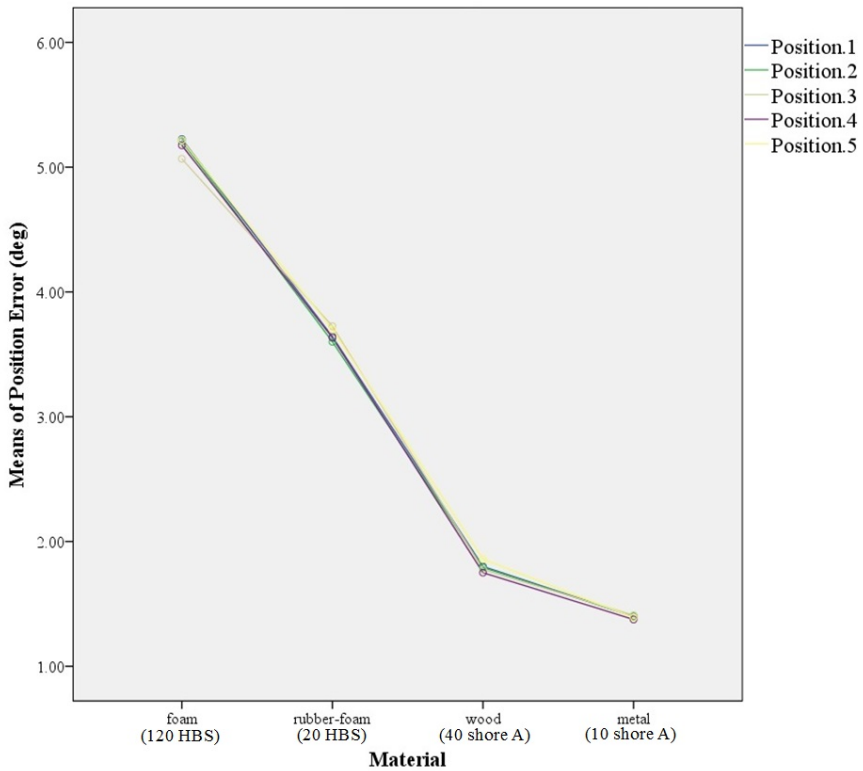

Figure 6.11. Position Error considering the Material and Position (Five different fixing positions to fix the sample materials) in human subject test.

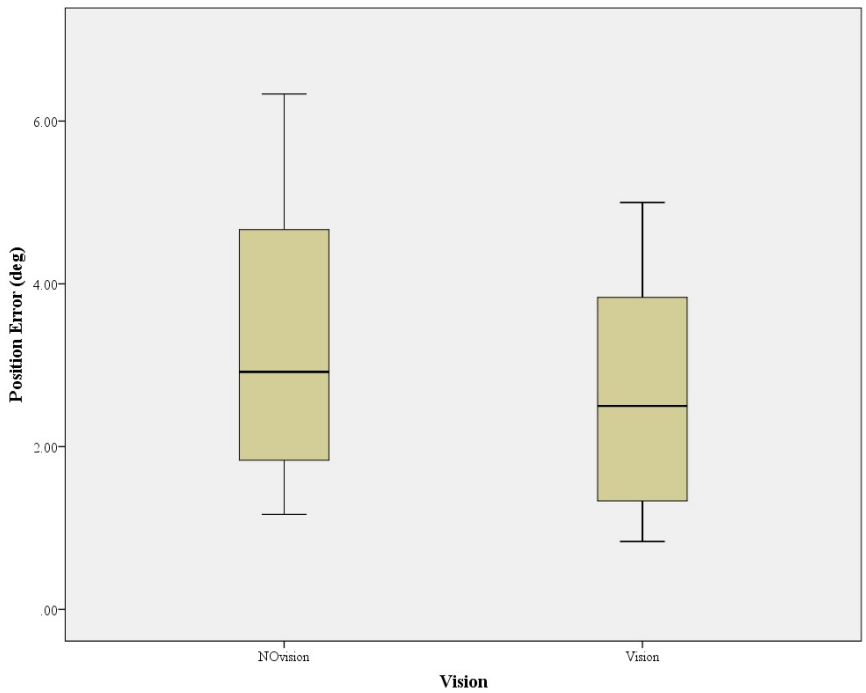

Figure 6.12. Position Error with visual feedback(vision) and without visual feedback(haptic feedback(Novision)).

7. CONCLUSION

In this study a contact sensory feedback method was provided for users of upper limb robotic prosthetic users. A tactor (as vibro-tactile haptic interface) has been designed to be attached on the shoulder to convey hardness feeling.

Acceleration response signals due to tapping on different materials containing important data about the hardness or softness of the materials which are tapped on. This fact was used in this study to provide hardness feeling of the materials which are touch by robotic prosthetic devices to the users. A tactor was designed to be attached on the shoulder and to play the acceleration response signals on the clavicle bone. The designed tactor was a voice coil motor attached to a plastic frame which could be fixed on the body using rubber straps.

Acceleration response of four different materials were collected and saved as look-up data after filtering with Infinite Impulse Response (IIR) filter. Signals were modeled using Auto Regressive Moving Average (ARMA) method. Cross Correlation of the recorded signals with modeled signals showed that those signals are similar to each other. In order to make the system to work in real-time an identification method has been developed using rate of the change of acceleration response signals.

An experimental setup has been developed for human subject study. The Purpose of the study was to understand whether the tactor is working well considering the provided feeling or not an also to realize if any delay is felt by the users in real time. The human subject study showed that hardness sensations provided by the tactor for different materials are significantly different with each other. In case of felt delay by the users results demonstrate that there is an small difference between only haptic feedback and only visual feedback.

Designed interface in this study could be also used in areas where thick gloves are desired to work in hot or dangerous environment. Further more, since sense of touch would be limited through these gloves, tactor designed in this study could be used to fedback contact information to the users. As future work the capability of the designed tactor to provide other sensations (slippage, surface roughness, ...) will be studied. Also it will be investigated to see whether a better design of the tactor, maybe smaller, could be produced.

APPENDIX A: STANDARD MECHANICAL PARTS

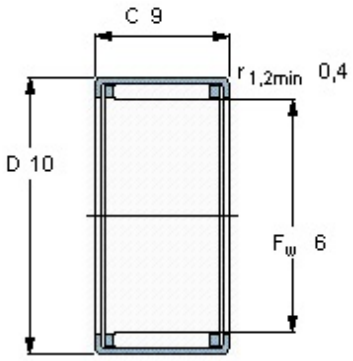

Figure A.1. Drawn cup needle roller bearings with open ends (HK0609).

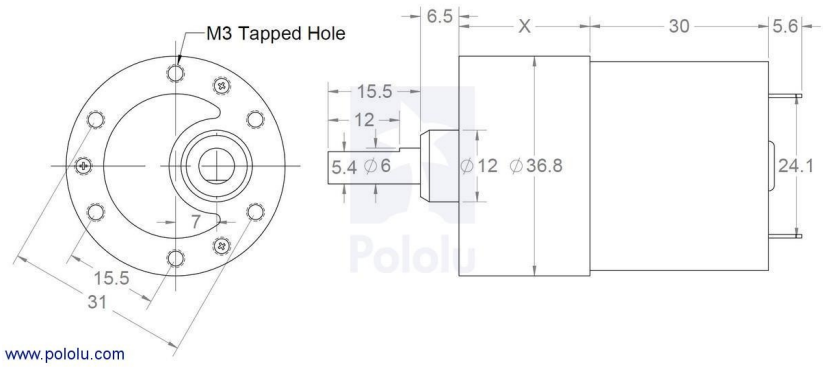

Figure A.2. Polulu 1447 DC motor.

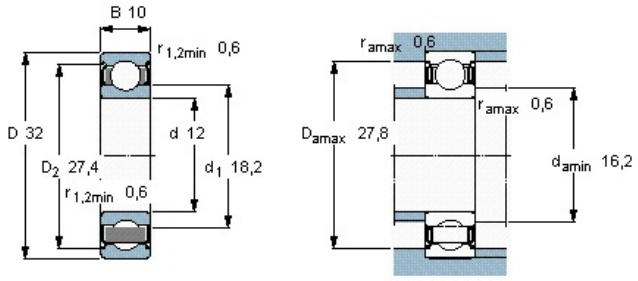

Figure A.3. Single row deep groove ball bearing SKF6201.

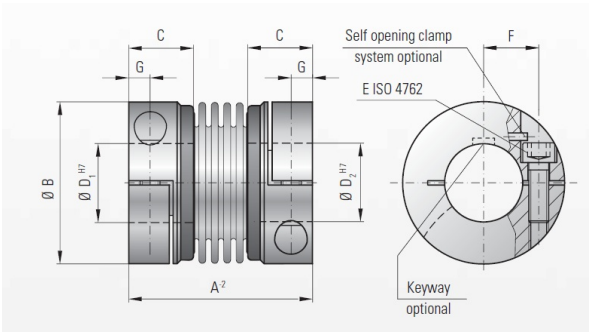

Figure A.4. R+k BKL 2.30.1 coupler: A=68 mm,B=56 mm, C=26 mm, D=10 mm, E=M6, F=20 mm, G=7.5 mm. The weight of coupler is 0.25 kg and it's torsional stiffness is 3193 Nm/rad.

APPENDIX B: STANDARD ELECTRICAL PARTS

The MCP4725 is a low-power, high accuracy, single channel, 12-bit buffered voltage output Digital-to-Analog Convertor (DAC) with non-volatile memory(EEPROM). The MCP4725 has a two-wire I2C^{TM} compatible serial interface for standard (100 kHz), fast (400 kHz), or high speed (3.4 MHz) mode.

DM74LS241 buffer/line driver is designed to improve both the performance and PC board density of 3-STATE buffers/ drivers employed as memory-address drivers, clock drivers, and bus-oriented transmitters/receivers. Featuring 400 mV of hysteresis at each low current PNP data line input, this chip provide improved noise rejection and high fanout outputs and can be used to drive terminated lines down to 133 Ω.

Main electrical circuit for capturing acceleration response signals and sending data to Tactor:

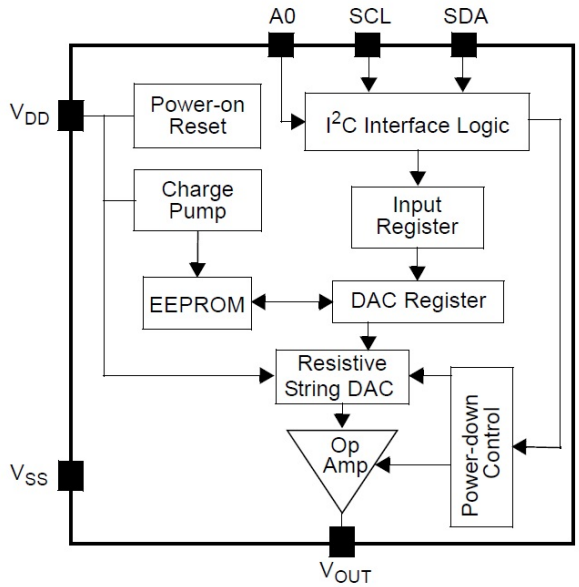

Figure B.1. MCP4725 Digital-to-Analog Convertor (DAC) from MICROCHIP CO.

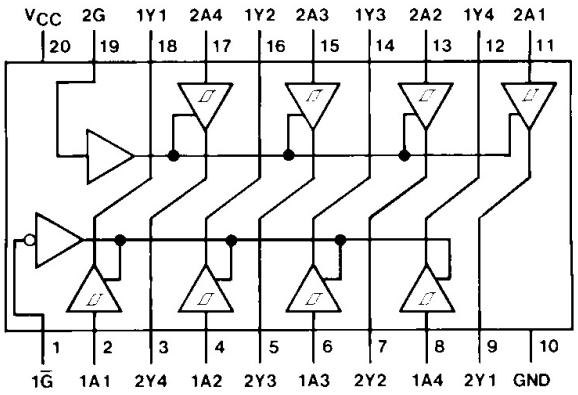

Figure B.2. DM74LS241 buffer from FAIRCHILD CO.

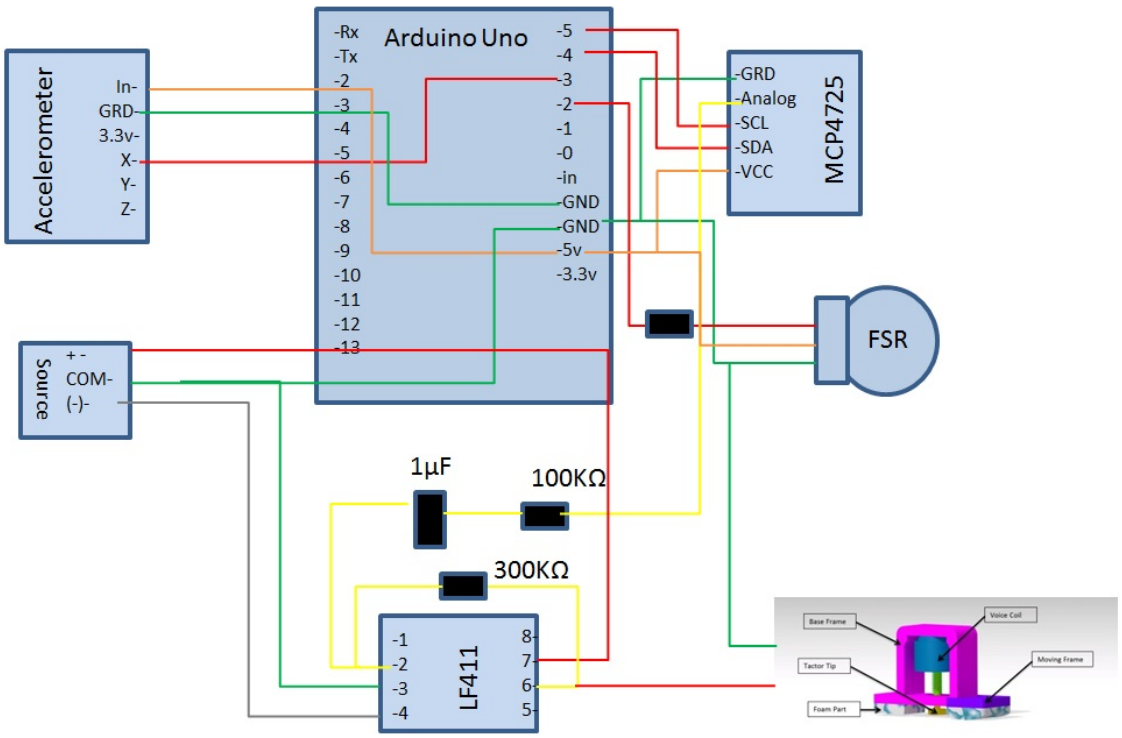

Figure B.3. Main electrical circuit.

REFERENCES

1. E. Gardner, J. Martin, T. j., "The Somatosensory System: Receptors and Central Pathways", *Principles of Neural Science*, chap. The Somato, pp. 431–437, Elsevier, 2000.

2. Pallasmaa, J., *The Eyes of the Skin: Architecture and the Senses*, Wiley-Academi, 2005.

3. Clippinger, F., R. Avery and B.Titus, "A sensory feedback system for an upper-limb amputation prosthesis", *Bulletin of Prosthetics Research*, Vol. 10, pp. 247–258, 1974.

4. Zecca, M., S. Micera, M. C. Carrozza and P. Dario, "Control of multifunctional prosthetic hands by processing the electromyographic signal.", *Critical reviews in biomedical engineering*, Vol. 30, No. 4-6, pp. 459–85, 2002.

5. Karl, A. and H. Flor, "Reorganization of motor and somatosensory cortex in upper extremity amputees with phantom limb pain.", *The Journal of neuroscience : the official journal of the Society for Neuroscience*, Vol. 21, No. 10, pp. 3609–18, 2001.

6. Dhillon, G. and H.Kenneth, "Direct neural sensory feedback and control of a prosthetic arm.", *IEEE transactions on neural systems and rehabilitation engineering : a publication of the IEEE Engineering in Medicine and Biology Society*, Vol. 13, No. 4, pp. 468–72, 2005.

7. Massimino, M. J. and T. B. Sheridan, "Sensory substitution for force feedback in teleoperation", *Presence*, Vol. 2, No. 4, pp. 344–352, 1993.

8. Bark, K., J. W. Wheeler, S. Premakumar and M. R. Cutkosky, "Comparison of Skin Stretch and Vibrotactile Stimulation for Feedback of Proprioceptive Information",

2008 Symposium on Haptic Interfaces for Virtual Environment and Teleoperator Systems, pp. 71–78, 2008.

9. El Kady, A., M. T., "A shape memory alloy actuated anthropomorphic prosthetic hand : initial experiments", *Middle East Conference on Biomedical Enginerring*, pp. 41–44, 2011.

10. El Kady, A., A. Mahfouz and M. Taher, "Mechanical design of an anthropomorphic prosthetic hand for shape memory alloy actuation", *2010 5th Cairo International Biomedical Engineering Conference*, pp. 86–89, 2010.

11. Toole, K., M. Mcgrath and E. Coyle, "Analysis and Evaluation of the Dynamic Performance of SMA Actuators for Prosthetic Hand Design Actuators for Prosthetic Hand Design", *Doublin Institute of Technology*, 2009.

12. Andrianesis, K. and A. Tzes, "Design of an anthropomorphic prosthetic hand driven by Shape Memory Alloy actuators", *2008 2nd IEEE RAS & EMBS International Conference on Biomedical Robotics and Biomechatronics*, pp. 517–522, 2008.

13. Toole, K., M. Mcgrath and M. Hatchett, "Transient characterisation and analysis of shape memory alloy wire bundles for the actuation of finger joints in prosthesis design", *Proceeding of Mechanika*, Vol. 6, No. 6, pp. 65–69, 2007.

14. Cipriani, C., M. Controzzi and M. C. Carrozza, "Progress towards the development of the SmartHand transradial prosthesis", *2009 IEEE International Conference on Rehabilitation Robotics*, pp. 682–687, 2009.

15. Ozawa, R., K. Hashirii and H. Kobayashi, "Design and control of underactuated tendon-driven mechanisms", *2009 IEEE International Conference on Robotics and Automation*, pp. 1522–1527, 2009.

16. Massa, B., S. Roccella, M. C. Carrozza and P. Dario, "Design and Development of an Underactuated Prosthetic Hand", *IEEE International Conference onRobotics & Automation*, pp. 3374–3379, 2002.

17. Cloutier, A. and J. Yang, "Control of Hand Prosthesis-A Literature Review", *ASME 2013 International Design Engineering Technical Conferences and Computers and Information in Engineering Conference*, pp. 1–11, 2013.

18. Navarro, X., T. B. Krueger, N. Lago, S. Micera, T. Stieglit and P. Dario, "A Critical Review of Interfaces with the Peripheral Nervous System for the Control of Neuroprostheses and Hybrid Bionic Systems", *Journal of the Peripheral Nervous System*, Vol. 10, pp. 229–258, 2005.

19. Battye, C., A. Nightingale and J. Willis, "The use of myoelectric currents in the operation of prostheses", *Journal of Bone and Joint Surgery*, Vol. 37-B, pp. 506–510, 1955.

20. Cranny, a., D. P. J. Cotton, P. H. Chappell, S. P. Beeby and N. M. White, "Thick-film force, slip and temperature sensors for a prosthetic hand", *Measurement Science and Technology*, Vol. 16, No. 4, pp. 931–941, 2005.

21. Prior, R., J. Lyman, Philip A . Case and C. Scott, "Supplemental sensory feedback for the va/nu myoelectric hand background and preliminary design", *Bulletin of Prosthetics Research*, Vol. 101, No. 134, pp. 170–191, 1976.

22. Childress, D., "Closed-loop control in prosthetic systems: historical perspective", *Annals of Biomedical Engineering*, Vol. 8, pp. 293–303, 1980.

23. Peckham, P. H. and D. B. Gray, "Functional neuromuscular stimulation (FNS)", *Journal of Rehabilitation Research and Development*, pp. 1–3, 1994.

24. Scott, R., "Feedback in myoelectric prostheses", *Clin. Orthop. Relat. Res.*, Vol.

256, pp. 58–63, 1990.

25. Shannon, G., "A comparison of alternative means of providing sensory feedback on upper limbProstheses", *Med Biol Eng*, pp. 289–294, 1976.

26. Anugolu, M., C. Potluri, A. Ilyas, P. Kumar, S. Chiu, N. Devine, A. Urfer, M. P. Schoen and S. M. Ieee, "A REVIEW ON SENSORY FEEDBACK FOR SEMG BASED", *International Conference on Artificial Intelligence*, 2011.

27. Kaczmarek, K. a., J. G. Webster, P. Bach-y Rita and W. J. Tompkins, "Electrotactile and vibrotactile displays for sensory substitution systems.", *IEEE transactions on bio-medical engineering*, Vol. 38, No. 1, pp. 1–16, 1991.

28. Shannon, G., "A Myoelectrically-Controlled Prosthesis with Sensory Feedback", *Medical and Biological Engineering and Computing*, pp. 73–80, 1979.

29. Kim, K., A. Member, J. E. Colgate, J. J. Santos-munn, A. Makhlin and M. A. Peshkin, "On the Design of Miniature Haptic Devices for Upper Extremity Prosthetics", *Transactions on Mechatronics*, Vol. 15, No. 1, pp. 27–39, 2010.

30. Scott, R., R. Brittain, R. Caldwell, A. Cameron and V. Dunfield, "Sensory feedback system compatible with myoelectric control.", *Journal Medical & Biological Engineering & Computing*, Vol. 18, pp. 65–69, 1980.

31. Sasaki, Y., Y. Nakayama and M. Yoshida, "Sensory feedback system using interferential current for EMG prosthetic hand", *Proceedings of the Second Joint 24th Annual Conference and the Annual Fall Meeting of the Biomedical Engineering Society*, Vol. 2, pp. 2402–2403, 2002.

32. Paciga, J. E., D. A. Gibson, R. Gillespie and R. N. Scott, "Clinical Eva uation of UNB 3-State Myoelectric Control for Arm Prostheses", *Bulletin of Prosthetics Research*, Vol. 17, pp. 21–33, 1980.

33. Brewster, S. and L. M. Brown, "Tactons : Structured Tactile Messages for Non-Visual Information Display", *Conferences in Research and Practice in Information Technology*, 2001.

34. Conzelman, J. E., S. Madre, H. B. Ellis, L. Canada and C. W. O'Brien, "Prosthetic Device Sensory Attachment", , 1953.

35. Bach-y Rita, P. and C. Collins, "Sensory substitution and limb prosthesis.", *Proceedings of the Third International Symposium on Advances in External Control of Human Extremities*, pp. 9–21, 1970.

36. Mann, R. and S. Reimers, "Kinesthetic sensing for the EMG controlled Boston Arm", *IEEE Trans. Man–Mach. Syst.*, Vol. 11, No. March, pp. 110–115, 1970.

37. Stepp, C. and Y. Matsuoka, "Relative to direct haptic feedback, remote vibrotactile feedback improves but slows object manipulation.", *Conf. Proc. IEEE Eng. Med. Biol. Soc.*, pp. 2089–2092, 2010.

38. Kuchenbecker, K. J., J. Fiene and G. Niemeyer, "Improving contact realism through event-based haptic feedback.", *IEEE transactions on visualization and computer graphics*, Vol. 12, No. 2, pp. 219–30, 2006.

39. Okamura, A., J. T. Dennerlein and R. D. Howe, "Vibration feedback models for virtual environments", *Proceedings. 1998 IEEE International Conference on Robotics and Automation (Cat. No.98CH36146)*, Vol. 1, pp. 674–679, 1998.

40. Massie, T. H. and J. K. Salisbury, "The PHANToM Haptic Interface : A Device for Probing Virtual Objects", *Dynamic Systems and Control*, Vol. 1, pp. 295–301, 1994.

41. Okamura, A. M., A. Member, M. R. Cutkosky and J. T. Dennerlein, "Reality-Based Models for Vibration Feedback in Virtual Environments", *IEEE/ASME*

TRANSACTIONS ON MECHATRONICS, Vol. 6, No. 3, pp. 245–252, 2001.

42. Romano, J. M., S. Member and K. J. Kuchenbecker, "Creating Realistic Virtual Textures from Contact Acceleration Data", *IEEE TRANSACTIONS ON HAPTICS*, Vol. 5, No. 2, pp. 109–119, 2012.

43. Aulignac, D., R. Balaniuk and C. Laugier, "A Haptic Interface for a Virtual Exam of the Human Thigh", *Proceedings of the 2000 IEEE lntemational Conference on Robotics 8 Automation*, pp. 2452–2457, 2000.

44. Campion, G. and V. Hayward, "Fundamental Limits in the Rendering of Virtual Haptic Textures", *First Joint Eurohaptics Conference and Symposium on Haptic Interfaces for Virtual Environment and Teleoperator Systems*, , No. 1, pp. 263–270, 2005.

45. Kontarinis, D. A. and R. D. Howe, "Tactile Display of Vibratory Information in Teleoperation and Virtual Environments", *Presence*, Vol. 4, No. 4, pp. 387–402, 1995.

46. Mcmahan, W., S. Member, J. Gewirtz, D. Standish, P. Martin, J. A. Kunkel, M. Lilavois, A. Wedmid, D. I. Lee and K. J. Kuchenbecker, "Tool Contact Acceleration Feedback for Telerobotic Surgery", *IEEE TRANSACTIONS ON HAPTICS*, Vol. 4, No. 3, pp. 210–220, 2011.

47. Yao, H.-Y., V. Hayward and R. E. Ellis, "A tactile enhancement instrument for minimally invasive surgery.", *Computer aided surgery : official journal of the International Society for Computer Aided Surgery*, Vol. 10, No. 4, pp. 233–239, 2005.

48. Kuchenbecker, K. J. and G. Niemeyer, "Induced Master Motion in Force-Reflecting Teleoperation", *Journal of Dynamic Systems, Measurement, and Control*, Vol. 128, No. 4, p. 800, 2006.

49. Bark, K., W. McMahan, A. Remington, J. Gewirtz, A. Wedmid, D. I. Lee and K. J. Kuchenbecker, "In vivo validation of a system for haptic feedback of tool vibrations in robotic surgery.", *Surgical endoscopy*, Vol. 27, No. 2, pp. 656–664, 2013.

50. Becker, T., J. During and A. Den Hertog, "Artificial Touch in a Hand Prosthesis", *Medical and Biological Engineering,*, Vol. 5, pp. 47–49, 1967.

51. Meek, S. G., S. C. Jacobsen and P. P. Goulding, "Extended physiologic taction: design and evaluation of a proportional force feedback system.", *Journal of rehabilitation research and development*, Vol. 26, No. 3, pp. 53–62, 1989.

52. Pylatiuk, C., A. Kargov and S. Schulz, "Design and Evaluation of a Low-Cost Force Feedback System for Myoelectric Prosthetic Hands", *JPO Journal of Prosthetics and Orthotics*, Vol. 18, pp. 57–61, 2006.

53. Chatterjee, A., P. Chaubey, J. Martin and N. V. Thakor, "Quantifying Prosthesis Control Improvements Using a Vibrotactile Representation of Grip Force", *2008 IEEE Region 5 Conference*, pp. 1–5, 2008.

54. Kuiken, T. a., L. a. Miller, R. D. Lipschutz, B. a. Lock, K. Stubblefield, P. D. Marasco, P. Zhou and G. a. Dumanian, "Targeted reinnervation for enhanced prosthetic arm function in a woman with a proximal amputation: a case study.", *Lancet*, Vol. 369, No. 9559, pp. 371–380, 2007.

55. Marasco, P. D., K. Kim, J. E. Colgate, M. a. Peshkin and T. a. Kuiken, "Robotic touch shifts perception of embodiment to a prosthesis in targeted reinnervation amputees.", *Brain : a journal of neurology*, Vol. 134, No. Pt 3, pp. 747–758, 2011.

56. Cipriani, C., M. D'Alonzo and M. C. Carrozza, "A miniature vibrotactile sensory substitution device for multifingered hand prosthetics.", *IEEE transactions on biomedical engineering*, Vol. 59, No. 2, pp. 400–408, 2012.

57. Witteveen, H. J. B., E. a. Droog, J. S. Rietman and P. H. Veltink, "Vibro- and electrotactile user feedback on hand opening for myoelectric forearm prostheses.", *IEEE transactions on bio-medical engineering*, Vol. 59, No. 8, pp. 2219–2226, 2012.

58. Damian, D. D., M. Ludersdorfer, A. Hernandez Arieta, R. Pfeifer and A. M. Okamura, "Wearable haptic device for cutaneous force and slip speed display", *2012 IEEE International Conference on Robotics and Automation*, pp. 1038–1043, 2012.

59. McMahan, W., J. M. Romano, A. M. Abdul Rahuman and K. J. Kuchenbecker, "High frequency acceleration feedback significantly increases the realism of haptically rendered textured surfaces", *2010 IEEE Haptics Symposium*, pp. 141–148, 2010.

60. Martin, G. H., *Kinematics and Dynamics of Machines*, McGraw-Hill, 1982.

61. Ogata, K., *Modern Control Engineering*, Prentice Hall PTR, Upper Saddle River, NJ, USA, 2001.

62. Isermann, R. and M. Munchhof, *Identification of dynamic systems : an introduction with applications*, Springer, 2011.

63. Kumar, P. R. and P. Varaiya, *Stochastic Systems : Estimation , Identification , and Adaptive Control*, 1986.

64. Mcbean, J. and C. Breazeal, "Voice Coil Actuators for Human-Robot Interaction", *Proceedings. 2004 IEEE/RSJ International Conference on Intelligent Robots and Systems, 2004. (IROS 2004).*, Vol. 1, pp. 852–858, 2004.

65. Zuowu, T., L. Jinfu and Y. Jialing, *Reciprocating Motor*, Beijing Press, 1991.

66. Goh, T. and B. Chen, "Design and implementation of a hard disk drive servo system using robust and perfect tracking approach", *IEEE Transactions on Control*

Systems Technology, Vol. 9, No. 2, pp. 221–233, 2001.

67. Peng, K., B. M. Chen, S. Member, G. Cheng, S. Member and T. H. Lee, "Modeling and Compensation of Nonlinearities and Friction in a Micro Hard Disk Drive Servo System With Nonlinear Feedback Control", Vol. 13, No. 5, pp. 708–721, 2005.

68. Feng, X., Z. Duan, Y. Fu, a.L. Sun and D. Zhang, "The technology and application of voice coil actuator", *2011 Second International Conference on Mechanic Automation and Control Engineering*, pp. 892–895, 2011.

69. Park, K., W. Youm and J. Jong, "Vibration reduction control of a Voice Coil Motor (VCM) nano scanner", *2007 7th IEEE Conference on Nanotechnology (IEEE NANO)*, Vol. 1, No. Vcm, pp. 520–523, 2007.

70. Aziziaghdam, M. and E. Samur, "Providing contact sensory feedback for upper limb robotic prosthesis", *2014 IEEE Haptics Symposium (HAPTICS)*, pp. 575–579, 2014.

71. Okamoto, S., M. Konyo, S. Saga and S. Tadokoro, "Identification of cutaneous detection thresholds against time-delay stimuli for tactile displays", *2008 IEEE International Conference on Robotics and Automation*, pp. 220–225, 2008.

72. Hwang, I., J. Seo, M. Kim and S. Choi, "Perceived intensity of tool-transmitted vibration: Effects of amplitude and frequency", *2012 IEEE International Workshop on Haptic Audio Visual Environments and Games (HAVE 2012) Proceedings*, pp. 1–6, 2012.

73. Ryu, J., J. Jung, S. Kim and S. Choi, "Perceptually Transparent Vibration Rendering Using a Vibration Motor for Haptic Interaction", *RO-MAN 2007 - The 16th IEEE International Symposium on Robot and Human Interactive Communication*, pp. 310–315, 2007.

74. Drewing, K., A. Ramisch and F. Bayer, "Haptic, visual and visuo-haptic softness judgments for objects with deformable surfaces", *World Haptics 2009 - Third Joint EuroHaptics conference and Symposium on Haptic Interfaces for Virtual Environment and Teleoperator Systems*, pp. 640–645, 2009.

75. Gescheider, G. A., *Psychophysics: the Fundamentals*, Lawrence Erlbaum Associates, Inc., 1997.

76. Yussof, H. and M. Ohka, "Application of stiffness control algorithm for dexterous robot grasping using optical three-axis tactile sensor system", *2009 International Symposium on Micro-NanoMechatronics and Human Science*, pp. 472–476, 2009.

77. Lamotte, R. H., "Softness Discrimination With a Tool Softness Discrimination With a Tool", pp. 1777–1786, 2000.

78. Aboul-Hagag, K. E., S. a. Mohamed, M. a. Hilal and E. a. Mohamed, "Determination of sex from hand dimensions and index/ring finger length ratio in Upper Egyptians", *Egyptian Journal of Forensic Sciences*, Vol. 1, No. 2, pp. 80–86, 2011.